=== **REVIEWS** ===

Mechanisms of Stress Generation in Thin Films and Coatings

A. R. Shugurov[a],* and A. V. Panin[a]

[a] Institute of Strength Physics and Materials Science, Siberian Branch, Russian Academy of Sciences,
Tomsk, 634055 Russia
***e-mail: shugurov@ispms.tsc.ru**

Abstract—Analysis of the literature data on the reasons for the development of mechanical stresses in epitaxial, polycrystalline, and amorphous films during their formation and under various external influences is carried out. The mechanism of the appearance of internal stresses during heteroepitaxial growth of films caused by the mismatch of the crystal lattice constants of the film and substrate is described. The relationship between the development of mismatch stresses in heteroepitaxial films and changes in the nature of their growth is shown. Models of the occurrence of compressive and tensile stresses in polycrystalline films due to the formation and coalescence of islands at the initial stage of their growth are considered. The regularities of the evolution of internal stresses in continuous films are discussed depending on the conditions of their deposition, as well as their chemical composition, structure, and mechanical properties. The mechanisms of development of internal stresses in thin films associated with the formation of point defects in them, the incorporation of impurities, and phase transformations occurring in the deposition process are reviewed. External factors that lead to the appearance of stresses in thin films during their storage and operation are considered in detail.

INTRODUCTION

Thin films are increasingly used in various fields of science and technology. They are used as functional coatings that significantly increase the hardness, wear resistance, and corrosion and thermal resistance of structural materials in the aerospace, mechanical engineering, energy, medicine, and chemical industries, as well as serving as the main structural element of various instruments and devices in micro- and nanoelectronics, solar energetics, optoelectronics, medicine, etc. At the same time, even in the case when thin-film structures do not require high strength to perform their main functions, the mechanical stresses that develop in them during deposition and during operation are one of the most important factors that affect their operational characteristics, reliability and durability. Tensile stresses can cause damage of the films by means of their cracking, peeling off the substrate, and chipping (Fig. 1a) [1–5]. Compressive stresses can also contribute to the edge peeling and chipping of films [6, 7] or lead to their buckling, blistering or wrinkling (Figs. 1b, 1c) [8–12]. In addition, stresses can cause changes in the chemical composition and internal microstructure of films [13–18], as well as also significantly affect their mechanical [19–21], tribological [22–25], electrical [25–29], magnetic

[30–32], optical [33–35], piezoelectric [36], and corrosive properties [37]; biosensitivity [38]; etc.

Mechanical stresses that occur in thin films can be divided into two groups [39]. The first group includes so-called "internal stresses" (stresses of growth), which develop directly during the formation of films and are caused by changes in their structure and chemical and phase composition that occur during their nucleation and growth. The second group includes external stresses arising in films after their deposition on the substrate due to changes in the temperature, chemical composition, and structure of the films; exposure to an electromagnetic field; and electromigration, as well as mechanical effects (tension, compression, bending); i.e., they are the result of action of any external forces on the film–substrate system.

The division of stresses into internal and external is rather arbitrary. The same factor can contribute to the development of stresses both during the growth of films and after their deposition. In addition, the relaxation processes that occur in films after deposition can lead to a change in their stressed state even in the absence of any external influences. However, such a classification allows a deeper understanding of the causes and mechanisms of stress development in films and coatings.
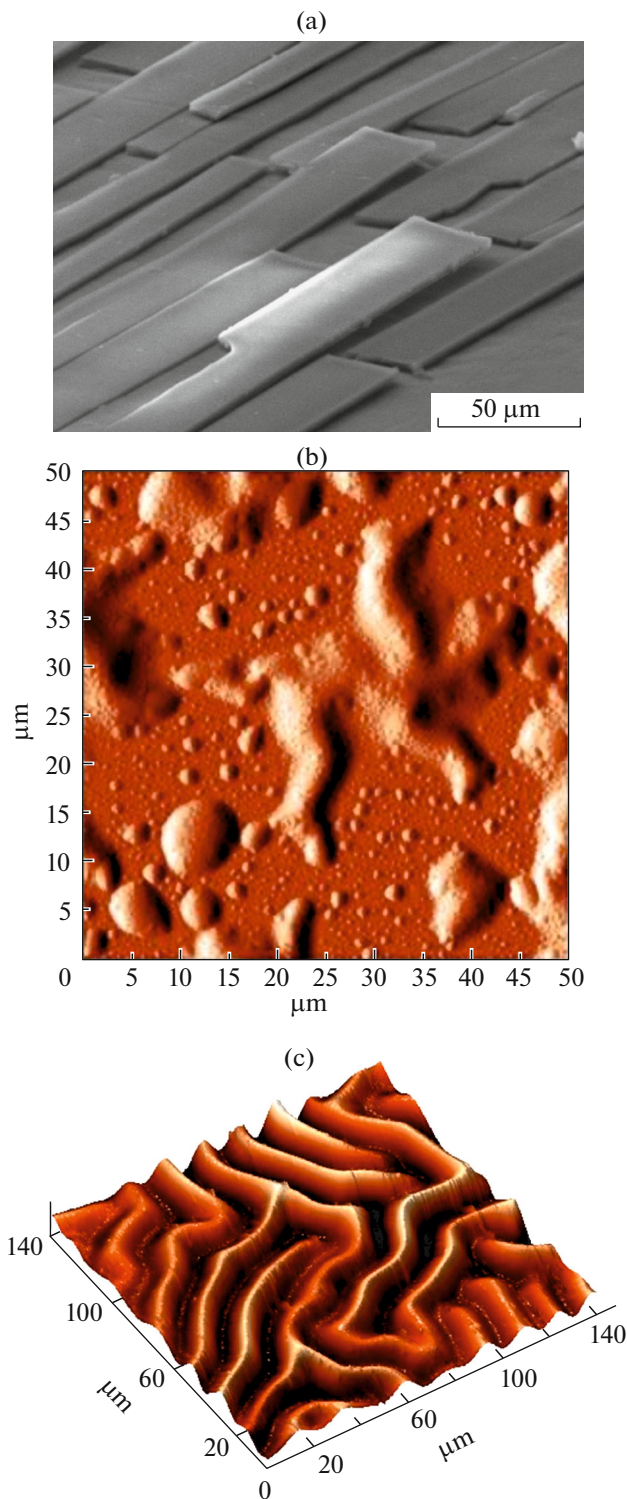
(a)

50 μm

(b)

(c)

Fig. 1. Deformation and destruction of thin films under stress: (a) cracking and chipping, (b) buckling, and (c) wrinkling .

Several factors can simultaneously act during the formation, storage, and operation of thin-film structures, contributing to the development of stresses in

them. The contribution of each of these factors to the total stress level significantly depends both on the materials of the film and substrate and on the impact conditions. Thus, when passing a high-density electric current through thin metal films, along with electromigration, heating due to the release of Joule heat, which depends on the rate of heat removal into the substrate, has a significant effect on the nature of the development of stresses in them. The contribution of various stress relaxation mechanisms to the deformation and destruction of thin films can also change accordingly. In addition, since various factors can cause the development of stresses of different signs in the films (compressive or tensile), their combined effect can contribute to both an increase and a decrease in the total stress level. Therefore, the analysis of the mechanisms of stress evolution in thin films is very important for developing effective methods for managing their stress states and, consequently, for improving the reliability and durability of thin-film structures.

This review systematizes and summarizes modern concepts of the fundamental physical mechanisms of the evolution of internal and external stresses in thin films. Analysis of the mechanisms of internal stresses is performed in Section 1. The factors that can contribute to the development of compressive and tensile stresses in both island and continuous films are discussed. The influence of the formation of point defects in thin films, the incorporation of impurities and phase transformations on the evolution of internal stresses in them is considered. The reasons for the development of thermal stresses in films, the mechanisms of stress development as a result of effects associated with the processes of electromigration, exposure to an electromagnetic field, and chemical and structural changes, as well as under various mechanical influences, are analyzed in detail in Section 2.

1. INTERNAL STRESSES

1.1. Mismatch Stresses in Epitaxial Films

The magnitude and sign of internal stresses in thin films depend on a number of factors, most of which are associated with the conditions and method of deposition of films on a substrate, as well as with the nature of their growth. Thus, during heteroepitaxial growth, when the materials of the film and the substrate are different, the appearance of internal stresses is mainly caused by the mismatch of the constants of their crystal lattices [40, 41]. On the surface of the substrate, there is a potential relief due to the distribution of atoms in the lattice sites. Therefore, it is energetically favorable for the initially single atoms of the deposited substance to be fixed in potential wells, completing the construction of the substrate lattice. However, as the density of atoms increases, the forces of their interatomic interaction arise, which tend to

arrange the film atoms in accordance with the lattice period characteristic of the given material. This is prevented by the bonding forces at the interface, as a result of which the internal stresses develop in the film and deformation of the film—substrate system occurs, at which the interatomic distances in the boundary layers of contacting materials become the same.

At the initial stage of growth, a continuous heteroepitaxial film is a stressed layer coherently conjugated to the substrate along the interface. If the parameters of the lattice of the film and the substrate differ insignificantly, then the pseudomorphic growth of the film, i.e., the adaptation of its crystal lattice to the lattice of the substrate material, can last rather enough. In this case, the Frank—van der Merwe mechanism of layer-by-layer growth of the film is realized [42, 43], in which a new layer of the deposited material begins to form only after the previous layer is formed (Fig. 2a). However, since elastic deformation energy of the film W is proportional to its volume V:

$$W = \frac{2\mu_f(1 + \nu_f)}{1 - \nu_f}\varepsilon^2 V \qquad (1)$$

(here, μ_f is the shear modulus, ν_f is the Poisson's ratio of the film, and ε is the plane deformation caused by mismatch stresses), an increase in the thickness of the growing layer leads to a rapid increase of W. It should be noted that the elastic relaxation due to the boundary conditions can lead to a significant decrease in the elastic energy in comparison with the value determined by (1). This effect is observed not only during layer-by-layer growth of films, but also in the case of structures that do not have a purely planar geometry [44].

Depending on the deposition conditions and characteristics of the film and substrate, the process of heteroepitaxial growth of the film can be accompanied by both elastic and plastic deformation [45—47]. If the plastic mechanism of relaxation of misfit stresses is realized, then germinating dislocations are formed in the film, which usually nucleate on its free surface. The propagation of these dislocations into the film leads to the formation of a network of misfit dislocations at its interface with the substrate.

Elastic relaxation of mismatch stresses can lead to coarsening of the surface of pseudomorphic films and the formation of a quasi-periodic relief [48]. A similar wrinkling relief, in particular, was observed on the surface of $La_{2x}Sr_xCuO_4$ films deposited on $SrTiO_3$ (100) substrates [49], as well as during the growth of GeSi films on a Si substrate [50]. In this case, the smaller the mismatch between the film and substrate lattices, i.e., the fewer the initial stresses in the film, the longer the wavelength of the folds (the average distance between neighboring folds) on its surface, and the later loss of stability of a smooth surface takes place.

In a smooth film, elastic stress relaxation can occur only through distortion, causing an increase in its
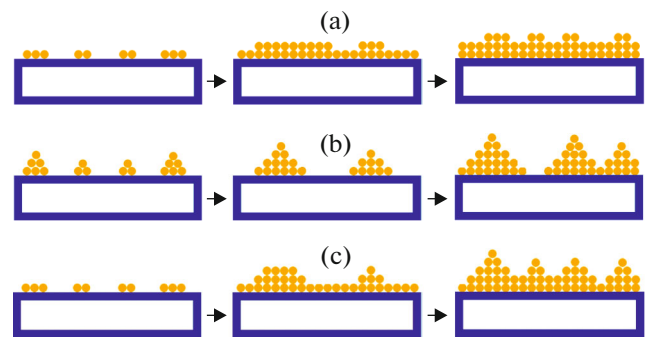

Fig. 2. Mechanisms of the formation of thin films: (a) Frank—van der Merwe regime (layer-by-layer growth), (b) Volmer—Weber mode (island growth), and (c) Stranski—Krastanov mode.

thickness, and, consequently, an increase of energy [51]. The appearance of irregularities of the film surface is a more effective mechanism of elastic relaxation, since it is possible to partially relax the lattice constant of the film plane to the equilibrium value. Stress relaxation through an increase of the film roughness reduces its free energy, but an increase of the surface area causes an increase of the surface energy. As was shown in [52—54], the smooth surface of a nonhydrostatically stressed solid is unstable with respect to disturbances with a certain wavelength, which is determined by the competition between its surface energy and the energy of deformation. Therefore, if elastic stress relaxation reduces the total free energy of the film, then folds appear on its surface, the height of which increases with time.

When the height of the folds becomes comparable to their wavelength, the formation of grooves begins between the folds, while the curvature of their surface decreases at the tops of the folds [55]. In the process of film growth, the grooves that develop under stress deepen and can form a pattern similar to cracking on the film surface [56], reaching the film/substrate interface, i.e., leading to a loss of film continuity. However, the evolution of grooves is quite rare in real heterosystems. A more frequent mechanism that provides elastic stress relaxation in epitaxial films is the decomposition of the film into separate islands.

Layer-by-layer growth of films (the Frank—van der Merwe mode) is realized when the wetting criterion is met, i.e., when the sum of surface energy of the film γ_f and energy of the film/substrate interface γ_i is less than surface energy of the substrate γ_s:

$$\gamma_f + \gamma_i < \gamma_s. \qquad (2)$$

In this case, the interaction forces at the film/substrate interface prevent the substrate surface from being exposed. If (2) is not satisfied, i.e., the film does not wet the substrate, then a continuous layer is not formed, with only separate islands appearing that are distributed over the substrate surface (Fig. 2b). This

growth mode is called the "Volmer–Weber mechanism" [57] and is realized, in particular, during the epitaxy of films of III–V compounds, for example, GaAs, on Si substrates [58]. Finally, a third mechanism of growth of heteroepitaxial films is possible, when, first, a wetting layer with a thickness of several monolayers grows on the surface of the substrate and, then, the growth of three-dimensional islands begins (Fig. 2c). Such a mechanism for the formation of epitaxial films is called the "Stranski–Krastanov mode" [59] and, in contrast to the Volmer–Weber mode, in this case, the film wets the substrate. However, strong internal stresses arising at a large (>2%) lattice mismatch between the film and the substrate prevent the maintaining of layer-by-layer growth. This mechanism is realized, in particular, when growing Ge films on Si substrates [60] and InAs films on GaAs substrates [61].

Modeling of heteroepitaxial growth in systems with a strong lattice mismatch, such as CdTe/GaAs or CdTe/Si, has shown that elastic stress relaxation is accompanied by the formation of either islands or V-shaped defects [62]. The mechanism of film surface roughening depends on the kinetic behavior of atoms on the surface of the growing layer, which is controlled by deformation. Almost complete relaxation of stresses occurs at the boundaries of atomic clusters, while the deformation energy increases significantly in their central part. Therefore, the atoms must move there for stress relaxation. However, since all neighboring places are occupied, relaxation is possible only through interlayer migrations, which leads to protrusions on the growing surface. Since there are no internal interfaces in single-crystal epitaxial films, the main mechanism of mass transfer in them is diffusion over the surface. Atoms move from one place on the surface to another, leading to a change in the free energy, which is determined by the gradient of the chemical potential along the surface. Thus, growth centers move along the surface to places with the lowest free energy, i.e., to the tops of protrusions, which causes the transit to the island growth mechanism.

1.2. Internal Stresses in Polycrystalline Films

One of the main reasons for the development of internal stresses in polycrystalline films is the evolution and densification of their structure during growth. In contrast to epitaxial films, polycrystalline films, as a rule, are formed under nonequilibrium conditions due to a high deposition rate and/or low substrate temperature. Under such conditions, the low mobility of adatoms on the substrate surface leads to the formation of a large number of nuclei and does not allow providing the preferential growth of crystallites with energetically favorable orientation. Therefore, polycrystalline films are almost always formed in accordance with the Volmer–Weber mechanism of island growth, which includes three consecutive stages:

nucleation and growth of three-dimensional islands (nuclei) of the deposited material on the substrate, their subsequent coalescence, and then the growth of a continuous film. In this case, at different stages of film growth, not only the magnitude, but also the sign of the internal stresses can change. In island films, as a rule, compressive stresses are observed [63]. Coalescence of islands, on the contrary, is accompanied by the development of tensile stresses [64]. Finally, in continuous films, depending on their material and deposition conditions, there can be both compressive and tensile stresses. Compressive stresses are usually observed in continuous films of materials with higher diffusion mobility (low melting point), such as Al, Cu, Ag, Au, etc. [65–68]. In turn, in films of materials characterized by low diffusion mobility (high melting point), for example, Fe, Cr, Mo, W, etc., as a rule, tensile stresses develop [66, 67, 69]. At the same time, the reverse situation may also occur under certain deposition conditions. For example, ion bombardment of films during growth significantly increases the diffusion mobility of adatoms, leading to the development of compressive stresses in films of materials with a high melting point [70]. On the contrary, a high deposition rate suppresses the diffusion mobility of adatoms, contributing to the appearance of tensile stresses in films of materials with a low melting point [71]. Below, the main mechanisms of stress evolution in polycrystalline films at various stages of their formation are considered in detail.

1.2.1. Compressive stresses in island films. Even at the initial stage of formation, when the islands are not in contact with each other, compressive stresses develop in them, the value of which can be very high. For example, in island Mo films deposited by magnetron sputtering on a Si substrate, the compressive stresses reached ~1 GPa [72]. In island diamond films on a graphite substrate, the compressive stresses exceeded 2.3 GPa [73].

The main factor leading to the appearance of compressive stresses in island films is the surface tension force, which tends to minimize the surface areas of the islands, which, as a result, acquire a convex shape with a positive surface curvature [63]. In accordance with Laplace's law, this causes the appearance of capillary pressure inside the island. For a spherical island, this additional pressure ΔP is defined as

$$\Delta P = \frac{2s}{R}, \tag{3}$$

where s is the surface tension force and R is the island radius (in the general case, for an island of arbitrary shape, the average radius of curvature of its surface is used instead of R). Since the pressure inside a convex island becomes higher, the equilibrium interatomic distance there decreases in comparison with a similar bulk material. As can be seen from (3), an increase in the island size during film growth should lead to a decrease in capillary pressure and, accordingly, to a

gradual increase of the lattice constant to its bulk value. However, after the island reaches a certain critical size, it is fixed on the substrate, which prevents further changes in the interatomic distances within it in the plane parallel to the film/substrate interface [74, 75]; therefore, the continued growth of islands contributes to their deformation along this plane, which, according to Hooke's law, is equal to

$$\varepsilon = -\frac{2s(1 - \nu_f)}{E_f R}, \qquad (4)$$

where E_f and ν_f are the elastic modulus and the Poisson's ratio of the film, respectively. Since for most low-index surfaces of metals and dielectrics $s > 0$, $\varepsilon < 0$, the compressive stresses develop in the islands. The estimation of internal stresses carried out in accordance with this approach showed that in island Au films on Al_2O_3 substrate, their value can reach 2 GPa [63], which is in agreement with the experimental data.

A mechanism has also been proposed according to which the presence of adatoms or some defects on the surface of the substrate and islands being formed can contribute to the development of compressive stresses [76, 77]. According to this mechanism, the interaction of adatom with the substrate surface leads to the formation of the field of elastic deformation in its surface layer, which can be considered as a "force dipole." This field causes the development of compressive stresses in islands, the growth of which is accompanied by continuous deposition of a large number of new adatoms. As a confirmation of the proposed mechanism, the authors in [77] point out that the value of compressive stresses in films decreases with a decrease in the flow of adatoms. The termination of the deposition process, i.e., the arrival of new adatoms, leads to a sharp decrease in the magnitude of the compressive stresses in the island films. In this case, a certain fraction of stresses remains unrelaxed, since they are caused by the action of surface tension forces considered above. However, detailed studies carried out by the molecular dynamics showed that the stresses associated with the presence of surface defects are significantly lower than the experimentally measured compressive stresses in island films [78].

1.2.2. Tensile stresses caused by island coalescence. As the size of the islands increases, they cover most of the surface of the substrate, and neighboring islands begin to interact with each other. This interaction results in coalescence, i.e., island merging, which is accompanied by the development of tensile stresses in the films [79−85]. The maximum value of these stresses σ_{max} significantly depends on the grain size at coalescence d_0 ($\sigma_{max} \sim 1/d_0$). In particular, at $d_0 \leq$ 10 nm, the stresses can reach several gigapascals [86].

The driving force of coalescence is a decrease in the total energy of the film when converting two free surfaces of islands into one grain boundary. The change in energy, in this case, can be written as

$$\Delta\gamma = 2\gamma_s - \gamma_{gb}, \qquad (5)$$

where γ_s is the surface energy and γ_{gb} is the energy of grain boundary. Since usually $2\gamma_s > \gamma_{gb}$, coalescence of islands is energetically favorable. For example, in the case of high-angle grain boundaries, when $\gamma_{gb} = (1/3)\gamma_s$ [87], the formation of a grain boundary provides an energy gain $\Delta\gamma = (5/3)\,\gamma_s$.

At the initial stage of coalescence, the growth of islands and filling of the free space between them is carried out through diffusion of adatoms over the surface of the islands and the surface of the substrate. However, when the distance between the islands becomes less than a certain critical value, the diffusion mechanism of filling the voids turns out to be difficult. It was suggested that the final stage of coalescence (corresponding to a deposited layer thickness of 10−50 nm), during which the islands become grains of a continuous film and boundaries are formed between them, is accompanied by the contraction of the space between the lateral faces of neighboring islands by means of their spontaneous elastic deformation [88, 89].

The model proposed in [88, 89] was further developed in [64]. It considers a regular array of hexagonal islands with a height of h and a transverse size of d on the substrate, which are located at distance Δ from each other until the coalescence process is completed (Fig. 3a). At this stage, the free energy of the island film per unit of its area can be written as [64]

$$W_1 = W_0 + \frac{4h\gamma_s}{d}, \qquad (6)$$

where W_0 is the contribution to the free energy of a unit of film area due to the upper face of the island and the film/substrate interface and γ_s is the surface energy of islands. The second term in (6) expresses the contribution to the free energy of the unit area of the film from the side faces of the islands. If the space between islands is contracted through elastic displacements of their side faces (Fig. 3b), then each island experiences biaxial deformation $\varepsilon = \Delta/d$. After completion of coalescence, the free energy of a unit area of a continuous film is equal to

$$W_2 = W_0 + \frac{2h\gamma_{gb}}{d} + \frac{E_f}{(1 - \nu_f)}\left(\frac{\Delta}{d}\right)^2, \qquad (7)$$

where the second and third terms are the free energy of grain boundaries and the energy of deformation per unit area of the film, respectively.

Expressions (6) and (7) make it possible to estimate the maximum width of the gap between the islands, which can be constricted due to their elastic deformation. For this, it is necessary to assume $W_2 = W_1$, since the contraction of the gaps becomes energetically unfavorable $W_2 > W_1$. As a result, it follows from (6) and (7) that
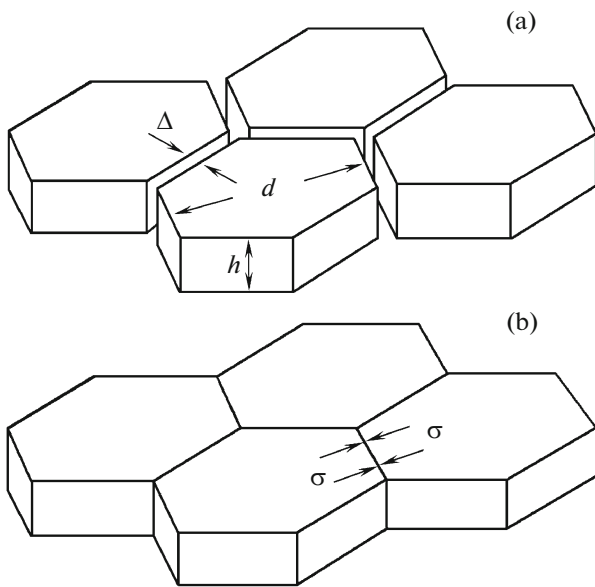
Fig. 3. Schematic representation of a polycrystalline thin film (a) before and (b) after coalescence of islands. Adapted from [64].

$$\Delta_{max} = \left[\frac{2d(1 - \nu_f)}{E_f}(2\gamma_s - \gamma_{gb}) \right]^{1/2}. \quad (8)$$

Accordingly, the maximum tensile stress in the film can reach

$$\sigma_{max} = \frac{E_f}{(1 - \nu_f)}\varepsilon_{max} = \frac{E_f}{(1 - \nu_f)}\frac{\Delta_{max}}{d}$$

$$= \left[\frac{2E_f}{(1 - \nu_f)d}(2\gamma_s - \gamma_{gb}) \right]^{1/2}. \quad (9)$$

Using the values of $E_f = 100$ GPa, $d = 10$ nm, $\gamma_s = 1$ J/m^2, and $\gamma_{gb} = 0.5$ J/m^2, one can find out that the elastic deformation of the islands makes it possible to constrict the gaps between islands up to 0.55 nm wide, while the maximum tensile stresses can reach 5.5 GPa. The obtained value is several times higher than the experimental values of stresses in polycrystalline films measured at the stage of coalescence of islands [79–85]. This discrepancy is especially large for films with a high diffusion mobility of adatoms (for example, for Au films deposited at room temperature). Obviously, this model is very simplified and contains a number of assumptions that do not correspond to reality. For example, it assumes that the walls of the islands are vertical and are able to interact with each other through the gap.

In [64], a more complex and physically realistic model was also proposed. In this model, filling the gap between neighboring islands and forming the grain boundary are considered from the standpoint of the Griffiths fracture criterion as a process of crack clo-sure. This model assumes the islands to have a rounded shape and their coalescence to begin with the occurrence of contact at one point. Thereafter, the zone between neighboring islands is considered as a crack, the closure of which is energetically advantageous, since it reduces the total free energy of the system (see (5)). In contrast to the model described above [89], in [64] it is assumed that the crack closure occurs gradually, accompanied by elementary acts of elastic deformation of islands until the decrease in surface energy due to the formation of the grain boundary exceeds the corresponding increase in the elastic deformation energy. Despite the significant differences between this mechanism of island coalescence and the model proposed in [89], the expression obtained in [64] for the average tensile stresses developing in the film differs from (9) only by the presence of $1 + \nu_f$ multiplier:

$$\sigma_{av} = \left[\frac{E_f}{(1 - \nu_f)}\frac{2(1 + \nu_f)}{d}(2\gamma_s - \gamma_{gb}) \right]^{1/2}. \quad (10)$$

It should be noted that the average stresses determined by (10) exceed the maximum stresses in (9); i.e., they turn out to be even more overestimated. Among the possible causes of such an overestimation, the authors [64] note that the model does not take into account the shear stresses that occur at the film/substrate interface when islands are deformed, as well as the assumption that the coalescence of all islands begins simultaneously.

Another approach to describing the mechanism of development of tensile stresses in thin films at the stage of island coalescence was proposed in [90]. The authors considered the coalescence of islands as a contact of elastic bodies between which the coupling force acts. This model is based on the classical Hertz theory of elastic contact of solids, taking into account the cohesive interaction between the contacting surfaces [91]. For three-dimensional islands of semispherical shape, the following expression is obtained in [90] for tensile stresses averaged over the volume of the island:

$$\sigma_{av} = \frac{4(2\gamma_s - \gamma_{gb})}{d}. \quad (11)$$

It is somewhat unexpected that, in accordance with this approach, the magnitude of stresses does not depend on the elastic properties of the material. Using the same parameter values as before ($d = 10$ nm, $\gamma_s = 1$ J/m^2, and $\gamma_{gb} = 0.5$ J/m^2), one can find that the tensile stresses in the films can reach 600 MPa. This value is in better agreement with the experimentally obtained values of stresses. However, this model does not allow explaining the large scatter of experimental data for different films, since the value determined by (11), in fact, can change only by varying the size of the islands.

1.2.3. Mechanisms of development of tensile stresses in continuous films. As was noted above, after the completion of island coalescence and the formation of a continuous film, one of the main factors determining the value of internal stresses in it is diffusion mobility of adatoms, which, in turn, depends on the homological temperature (the ratio of the film deposition temperature to its melting temperature T_d/T_m) and the deposition rate. In general, thin-film materials can be divided into two types [79–85, 92, 93]. The first type of films deposited at low homologous temperature ($T_d/T_m < 0.2$, for example, Fe, Cr, Ti, and Pt films deposited at room temperature) and/or high deposition rate are characterized by low diffusion mobility of adatoms. In these films, tensile stresses arising at the stage of island coalescence persist after its completion and increase with increasing thickness of the deposited layer (Fig. 4). Films of the second type are formed at higher homologous temperatures and/or low deposition rates. In these films, with an increase in thickness, there is a transition of tensile internal stresses into compressive ones, so that the maximum value of tensile stresses corresponds to the completion of coalescence of islands (Fig. 4). According to [85], the homologous temperature of films of the second type is on the order of 0.22–0.24 and higher. Thus, Au, Ag, and Cu demonstrate a high mobility of adatoms even at room temperature, whereas in the case of Ni films this requires a deposition temperature above 150°C. At the same time, the authors in [84] obtained Ti films, the evolution of internal stresses in which is typical for films of the second type already at a homological temperature of 0.15. A possible explanation for this may be the difference in the deposition rates of the films.

In contrast to films of the first type, the magnitude of tensile stresses in which does not change after the end of the deposition process, in films of the second type, the termination of deposition leads to a rapid relaxation of compressive stresses (within a few minutes after deposition). Under certain conditions, the reverse transition of compressive stresses into tensile stresses is even observed in them [92]. In this case, the resumption of film deposition again leads to the appearance of compressive stresses [84]. It was found that a similar character of the change in the magnitude and sign of internal stresses can take place even before the completion of the deposition process in the case of deposition of films at certain intermediate temperatures and deposition rates. In particular, in Ni films deposited in the temperature range from 27 to 150°C, after reaching a certain maximum value of compressive stresses, their relaxation began, which, at certain values of the deposition rate, ended with the repeated development of tensile stresses [85].

The evolution of internal stresses in continuous polycrystalline films is a very complex process, since it is controlled not only by the competition between dif-
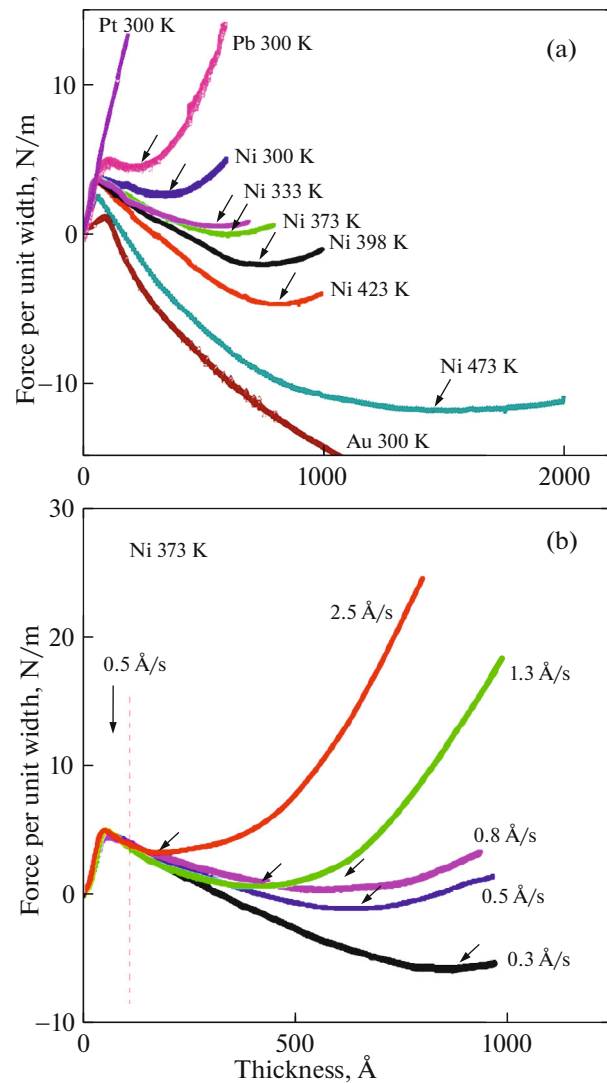
Fig. 4. Evolution of internal stresses in Pt, Pd, Au, and Ni films deposited (a) at different temperatures, and Ni films deposited (b) at different deposition rates. The arrows indicate the thickness of the films at which the change in the nature of stress changes occurs. Adapted from [85] by courtesy of Elsevier.

ferent mechanisms of stress development, but also by their competition with the simultaneously acting mechanisms of relaxation of these stresses. In this case, the contribution of these mechanisms to the total value of stresses depends significantly on the material of the films, as well as on the method and conditions of their deposition. To date, a number of different models have been proposed that describe the mechanisms of the development of tensile stresses in continuous polycrystalline films. The most important ones are discussed below.

An increase in tensile stresses in films of the first type after completion of island coalescence is usually explained by the fact that the upper layers of the film

grow epitaxially on the surface of already-formed grains, inheriting their nonequilibrium structure [64, 85, 92, 93]. In this case, the formation of grain boundaries continues in the newly deposited layers, the grains often have a columnar structure, so that the volume of the grain boundaries increases linearly with increasing film thickness. Therefore, tensile stresses continue to increase in accordance with the mechanism described above for the island coalescence stage.

Another mechanism for the development of tensile stresses is associated with recrystallization and grain growth occurring in a continuous film both during its deposition and after its completion [81, 86, 92–94]. This mechanism does not play a significant role in films of the first type, since in their case the low diffusion mobility of adatoms does not contribute to significant grain growth; however, it contributes to the relaxation of compressive stresses and the reappearance of tensile stresses in films of the second type, in which the mobility of adatoms is high.

Since the substrate does not have a significant orienting effect on the growth of polycrystalline films, the arrangement and crystallographic orientation of neighboring islands are random, which does not contribute to the formation of equilibrium boundaries when they merge. The nonequilibrium nature of the formation of polycrystalline films leads to the density of the material at the grain boundaries being lower than inside the grain. The grain boundaries contain excess free volume, which arises both as a result of an increase in the average distance between atoms in comparison with the equilibrium value and as a result of the formation of pores. For example, for FCC metals, the excess free volume per unit area of the grain boundary is $\Delta V \sim 1$ Å [95]. In the process of grain growth, the number of grain boundaries decreases and, consequently, this free volume is redistributed. As a result, the film becomes compacted, which in a free state would lead to a decrease in its size. However, since the film is rigidly bound with the substrate along the interface, it can only change its thickness. The transverse dimensions of the film remain unchanged, and it undergoes biaxial deformation, which, with an increase in the average grain size from d_0 to d, is [86]

$$\varepsilon_d = \Delta V \left(\frac{1}{d} - \frac{1}{d_0} \right). \qquad (12)$$

If this deformation is accommodated elastically, then the compaction of the film during grain growth causes the development of biaxial tensile stresses in it,

$$\sigma = \frac{E_f}{(1 - \nu_f)} \varepsilon_d \qquad (13)$$

and leads to an increase in its average energy density (energy per unit volume of the film) by the value

$$\Delta F_d = \frac{E_f}{(1 - \nu_f)} \varepsilon_d^2. \qquad (14)$$

From the above, in particular, it follows that tensile stresses in films can inhibit grain growth in them, since it turns out to be energetically unfavorable due to an additional increase in stresses and an increase in elastic energy. For sufficiently small d_0 ($d_0 \leq 4$ nm), a decrease in the energy density associated with a decrease in the number of grain boundaries per unit area of the film [86],

$$\Delta F_{gb} = \gamma_{gb} \left(\frac{2}{d_0} - \frac{2}{d} \right), \qquad (15)$$

may be less than ΔF_d. In this case, each stress value corresponds to a certain limiting grain size, upon reaching which the growth of grains in the film stops. Thus, calculations performed in [93] showed that stresses of 6 GPa stabilize the grain size in metal films at a level of 1.3 nm. If $\Delta F_{gb} \geq \Delta F_d$, then the grain growth will continue, leading to the development of strong deformations. In general, the presence of tensile stresses promotes the formation of fine-grained films, while compressive stresses, on the contrary, favor the growth of large grains.

It should be noted that the rate of increase in stresses that develop as a result of grain growth, as well as their total value, significantly depend on the initial grain size [94]. In the case of very small grains (~1 nm), which, as a rule, are observed only in discontinuous films, the stress growth rate is the highest and the stresses themselves can reach 1 GPa at room temperature. At the same time, for films with larger grains (~20 nm), the growth rate of stresses caused by grain growth is low, and their maximum value does not exceed 1 MPa. Thus, as was noted above, at a low diffusion mobility of adatoms, grain growth cannot lead to the development of strong internal stresses in continuous films. However, this mechanism of stress development becomes very important at a high diffusion mobility of adatoms, for example, in the case of film deposition at an elevated temperature.

Nonequilibrium of grain boundaries leads to the development of relaxation processes even in the case in which the grains in the film do not grow. The atoms at the grain boundaries tend to occupy equilibrium positions in order to lower the total free energy of the film, which leads to a redistribution of the excess free volume, i.e., the compaction of some regions and the appearance of porosity in others. Since the surface energy of the pore is always greater than the energy of the grain boundary, a driving force arises in the film, tending to tighten the pore. This causes the development of elastic deformations and tensile stresses in films in accordance with a mechanism similar to that described above for the coalescence of islands [64, 87–89]. Calculations performed in [94] show that, at small pore sizes and high density of their distribution over grain boundaries, relaxation processes developing there can lead to strong tensile stresses (up to 1 GPa) even at room temperature.

1.2.4. Mechanisms of development of compressive stresses in continuous films. In contrast to tensile stresses, the main mechanism of the occurrence of which in polycrystalline films is today considered to be the process of grain boundary formation described above, a complete understanding of the mechanisms of development of compressive stresses in films is currently lacking. A number of studies suggest that compressive stresses in continuous films are inherited from island films, in which, as noted above, they are the result of capillary forces [63, 81, 92, 96]. The authors of other articles [76, 77] believe that, as in island films, a "force dipole" mechanism acts during the growth of continuous films, which causes the compression of the film due to the interaction of adatoms with its surface. It is also assumed that compressive stresses in thin films may result from the incorporation of excess atoms between neighboring steps on a growing surface [97]. The recently proposed model assumes that stresses in continuous polycrystalline films arise as a result of the interaction of neighboring grains, which causes their deformation, including grain boundary sliding [98, 99].

The kinetic model, which describes the evolution of internal stresses in films and coatings on the basis of dynamic processes occurring during their growth at the atomic level [100−104] is of particular note. This model relates the mechanism of compressive stress development to the diffusion flow of atoms from the free surface of the growing film to the grain boundaries (Fig. 5). The driving force of this flow is the gradient of the chemical potential, which occurs due to the nonequilibrium of the deposition process and the increased concentration of adatoms on the film surface. A directed diffusion flow leads to excessive embedding of atoms at grain boundaries, i.e., to compaction of the film and the development of compressive stresses. At the stage of stable growth of a continuous film, when the length of grain boundaries grows at the same rate as the thickness of the film, the average stress in the latter, according to the kinetic model, can be written as [103]

$$\sigma_f = \sigma_c + (\sigma_t - \sigma_c)\exp(-\beta D/R_d d), \qquad (16)$$

where σ_c is the compressive stress caused by the embedding of atoms on grain boundaries; σ_t is the tensile stress caused by the formation of new areas of grains; β is a parameter that depends on the concentration of mobile adatoms on the film surface, the atomic volume and elastic modulus of the film material, and temperature; D is the effective diffusion coefficient of adatoms; R_d is the film deposition rate; and d is the grain size. The estimates showed that, for the development of stresses and deformations, which are usually observed during the growth of films of materials with high adatom mobility (deformation of about 0.1%), an increase in the chemical potential on the free surface of 0.15 kT is necessary [100]. This approximately corresponds to the embedding of one excess
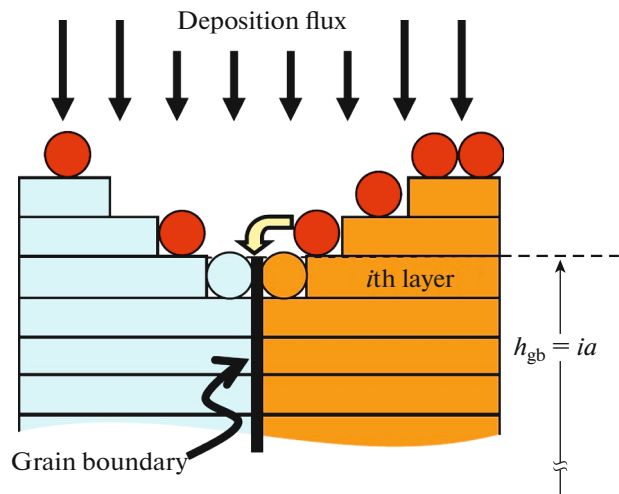
Fig. 5. Diagram illustrating the mechanism of development of compressive stresses in a polycrystalline thin film due to the diffusion of atoms from its surface to grain boundaries. Adapted from [102] by courtesy of Elsevier.

atom at the grain boundary during the growth of one monolayer of the film.

An advantage of the kinetic model is the fact that it considers their nonequilibrium nature as the main reason for the development of compressive stresses in polycrystalline films and directly relates the magnitude of the stresses to the parameters of deposition and microstructure of the films (see (16)). Therefore, it makes it easy to explain the dependence of the internal stress value on the temperature and the film deposition rate observed in experiments. At low temperature (or high deposition rate), the diffusion mobility of adatoms is very small and they are fixed on the free surface of the film. As follows from (16), $\sigma_f \approx \sigma_t$; i.e., only mechanisms of tensile stress generation operate in the film, mainly due to the formation of grain boundaries. On the contrary, at high temperature (or low deposition rate), surface diffusion and diffusion along grain boundaries can provide a mass transfer controlled by a gradient of the chemical potential from the free surface to the grain boundaries, resulting in the development of compressive stresses. Since compressive stresses act in the film plane, they gradually lead to an increase in the chemical potential at the grain boundaries. This process continues until the chemical potential at the grain boundaries becomes equal to the chemical potential at the surface of the film, i.e., until a quasi-equilibrium state is established. After that, the compressive stresses no longer grow, and simultaneously acting mechanisms of development of tensile stresses cause relaxation of compression. This pattern is observed in films deposited at intermediate homologous temperatures and deposi-

tion rates, in which compressive stresses begin to relax after reaching a certain film thickness (Fig. 4).

Another advantage of this model is that it allows one to explain the experimentally observed relaxation of compressive stresses in films after the termination of their deposition process [65, 105−107].

As soon as the flow of atoms deposited on the free surface of the film becomes zero, the chemical potential there decreases to an equilibrium value. At the same time, the chemical potential at grain boundaries remains elevated due to the accumulation of excess atoms. As a result, an oppositely directed gradient of the chemical potential arises, which causes a backflow of atoms from the grain boundaries to the free surface, leading to relaxation of compressive stresses. The resumption of film deposition again causes an increase in the chemical potential on the free surface of the film and a flow of atoms to the grain boundaries.

Recently, the kinetic model has been further developed to take into account the effect of grain growth during deposition of polycrystalline films on the evolution of internal stresses in them [108]. Two effects were considered: the development of stresses in the film due to changes in the microstructure of already formed layers, and the effect of increasing the initial grain size in newly deposited layers on the magnitude of stresses in them. The calculations performed showed good agreement with the experimental data, according to which the value of compressive stresses in films characterized by a significant increase in grain size during deposition continuously changes with increasing thickness of the deposited layer [85]. The analysis of the obtained data shows that the main reason for the change in the stress value in such films is not the evolution of the microstructure of the formed layers, but an increase in the transverse grain size in new layers of the film with an increase in its thickness. The latter lead to a gradual decrease in the length of grain boundaries per unit surface area of the film, which reduces the number of adatoms embedded on the grain boundaries, and, as a result, reduces compressive stresses.

The kinetic model showed good agreement with the evolution of internal stresses in Ni [109−111] and Cu [111−113] films obtained by electrolytic deposition. In particular, in these studies, a decrease in the magnitude of stresses was observed with an increase in the deposition rate and grain size, which directly follows from the kinetic model. It should be noted that the deposition of these films proceeded at a low homologous temperature, when diffusion processes in thin films are largely suppressed. It was shown in [65] that the degree of relaxation of compressive stresses in Au films after their deposition by chemical vapor is stopped decreases with an increase in the average grain size. This result also agrees well with the kinetic model, since a larger grain size corresponds to a shorter grain boundary length per unit surface area of

the film. Consequently, an increase in the grain size leads to a decrease in the number of atoms that can diffuse from the grain boundaries to the free surface of the film, leading to the relaxation of compressive stresses. Unfortunately, the dependence of the magnitude of developing compressive stresses on the grain size is not given in [65], which does not allow comparing the effect of grain boundaries on the development and relaxation of stresses. A recent analysis of the results of measuring the stresses in Ni films obtained by electron beam evaporation [85] carried out using a modified kinetic model that takes into account grain growth during film deposition showed that it is able to adequately describe the evolution of stresses in the case of films deposited at high homologous temperatures, when there is a high mobility of adatoms [108]. In particular, it made it possible to explain the dependence of the stresses in these films on temperature and the rate of their deposition.

At the same time, in [77], a significant difference was revealed between the relaxation rates of compressive stresses upon termination of the growth of Cu films and their repeated development after the resumption of the deposition process. The recovery of compressive stresses occurred one to two orders of magnitude faster than their relaxation, which is not fully consistent with the kinetic model, in which the flows of atoms directed to and from grain boundaries are assumed to be symmetric. On the other hand, the observed difference may be a consequence of the difference between the energies of newly deposited adatoms and atoms diffusing from grain boundaries, which significantly affects their diffusion mobility. Investigation of the evolution of internal stresses in thin Fe films deposited by electron-beam evaporation did not reveal a significant effect of the grain size on the value of internal stresses [114]. In this case, the degree of relaxation of compressive stresses after the termination of the deposition of films increased with an increase in their thickness. Such effects contradict not only the kinetic model, but also the mechanism of the development of compressive stresses as a result of the interaction of adatoms with the growth surface [76, 77]. The authors of [114] believe that the reversible stress relaxation in thin Fe films after the termination of their deposition is due to the rearrangement of the surface, which is controlled by surface diffusion. After stopping the deposition process, atoms diffuse from the more stressed central part of the grain to its boundaries, which lead to stress relaxation and surface smoothing. The resumption of growth causes the reverse process of surface roughening and the repeated development of compressive stresses.

Thus, despite a large number of experimental and theoretical studies that have been carried out, as well as numerous reviews of modern concepts of the causes and mechanisms of the development of internal stresses in thin polycrystalline films during growth [67, 69, 75, 92, 94, 97, 102, 115−119], today none of the

proposed models are capable of fully explaining all the experimentally observed regularities of their evolution. It is obvious that further experimental and theoretical studies are required to understand and take into account all the mechanisms of the occurrence and evolution of internal stresses in polycrystalline films. In this case, one of the most promising areas of these studies is the further development and validation of the kinetic model, which combines the mechanisms of development of tensile stresses due to the formation of grain boundaries [64] and compressive stresses due to the embedding of excess atoms at the grain boundaries [100].

1.3. Internal Stresses Due to the Formation of Defects in Films

Defects (interstitial atoms, vacancies, dislocations, etc.) formed in films during deposition make a significant contribution to the development of internal stresses in thin films and coatings, especially those obtained by sputtering or ion-assisted evaporation, based on the deposition of particles with high kinetic energy. The stresses caused by defects can reach very high values taking into account the simultaneous action of other mechanisms of stress development. For example, in TiN films deposited by high-power impulse magnetron sputtering, the value of residual compressive stresses exceeded 10 GPa [120, 121].

One of the important mechanisms of stress development in films deposited by methods using high-energy particles is the so-called "atomic (ion) peening" [122–124]. When colliding with a growing film, some of the adatoms can be incorporated in its surface layer, in the interstices of the crystal lattice. This leads to distortion of the crystal lattice and excessive compaction of the film. As a result, compressive stresses arise in it, the magnitude of which are directly proportional to the molar volume and the elastic modulus of the film [125]. Along with the atoms of the sputtered material, impurity atoms and ions, for example, ions of an inert gas used to bombard a target, can be incorporated into the interstices of the crystal lattice. "Atomic peening" predominantly occurs at low homologous temperatures, when the low diffusion mobility of adatoms does not allow them to move to equilibrium positions [69]. At a high homologous temperature, the incorporated atoms easily diffuse onto the free surface or onto the grain boundaries, as a result of which this mechanism does not significantly affect the development of stresses in the films. Another important parameter affecting the concentration of interstitial atoms and, thus, the magnitude of internal stresses in films obtained by the sputtering is the pressure in the working chamber [69, 126]. Under low-pressure conditions, most of the deposited atoms do not experience collisions with each other and, upon collision with the film surface, have high energy, which promotes their penetration into interstices and

the development of compressive stresses. On the contrary, at high pressures, atoms repeatedly collide with each other and with ions of the working gas, which leads to energy losses and a low concentration of point defects, as a result of which residual tensile stresses can arise in the films [126].

The development of compressive stresses in films due to "atomic peening" is significantly influenced by the bias voltage applied to the substrate [115, 127]. At high bias voltages, a strong electromagnetic field is created near the substrate surface, which accelerates the ions that bombard it. This leads to an increase in their kinetic energy and, as a consequence, increases the concentration of point defects in the film. Thus, tensile stresses developed in Cr films deposited at a bias voltage of up to 55 V [128]. At the same time, an increase in the bias voltage to 75 V and more led to the appearance of compressive stresses of 0.5−1 GPa in them, which were a consequence of "atomic peening."

High-energy atoms and ions can lead to the appearance in films not only of interstitial atoms, but also of substitutional atoms [115]. Such point defects are formed, for example, when sputtering composite films. In this case, if the substitution occurs by an atom having a larger radius than the lattice atom, then compressive stresses develop in the film. Otherwise, tensile stresses arise. The magnitude of these stresses can reach very high values. Thus, it has been shown that the substitution of 1 wt % of nitrogen atoms with titanium atoms in TiN films leads to the development of compressive stresses, the value of which reaches 4.1 GPa [129].

The depth of occurrence of point defects strongly depends on the energy of the bombarding particles. Modeling by molecular dynamics has shown that the bombardment of a copper substrate with Cu atoms requires an energy of 20 eV for the appearance of interstitial atoms [130]. In this case, these atoms penetrate into the second layer from the top layer of the substrate. An increase in the energy of incident atoms to 80 eV allowed them to penetrate into the third from the top layer of the substrate, while the depth at which interstitial atoms appeared reached 12 monolayers. In this case, displacements of the atoms developed through a chain of focused replacement collisions.

The models proposed for describing the mechanisms of stress development during the introduction of atoms and ions consider the deposited film as a matrix containing incorporated particles. In this case, the stress-deformed state of the film is a combination of hydrostatic stresses caused directly by the formation of a defect and biaxial stresses caused by restrictions on the change in dimensions imposed by the substrate on the film [129, 131−133]. In this case, hydrostatic and biaxial stresses have opposite signs; i.e., the hydrostatic expansion of the film due to the incorporation of a point defect causes biaxial compression in the plane of the film.

Recently, an extended kinetic model was proposed to describe the evolution of stresses in films obtained using high-energy particles [134]. Along with thermally activated diffusion processes on the surface and grain boundaries described in the kinetic model for low-energy deposition methods (see the previous section), the extended kinetic model also takes into account the role of point defects formed in films as a result of "atomic peening" in the development of internal stresses. According to this approach, the average stress in the film can be written as the sum of three terms:

$$\sigma_f = \sigma_{gr} + \sigma_{gb} + \sigma_b, \tag{17}$$

where σ_{gr} is the stress that develops during film growth, which is determined by (16); σ_{gb} is the stress caused by the compaction of the film due to the introduction of defects (atoms) in the regions adjacent to the grain boundaries; and σ_b is the stress associated with the embedding of defects into the volume of grains. The second and third terms in (17) are defined as [134]

$$\sigma_{gb} = A(l/d) \tag{18}$$

and

$$\sigma_b = (1 - l/d)\sigma_0 C_{ss}, \tag{19}$$

where A is the parameter depending on the energy and flow of the bombarding particles, as well as on the film growth rate; l is the depth of the defect penetration into the film; d is the grain size; σ_0 is the stress created in the film by one defect; and C_{ss} is the average concentration of defects in the film at the stage of steady growth.

Since the model considers only defects formed as a result of the introduction of excess atoms into the film, the last two terms in (17) represent compressive stresses. Their sum may exceed stresses σ_{gr} caused by thermally activated diffusion processes in the growing film, so total stress σ_f will also be compressive [118, 134]. This makes it possible to explain why compressive stresses often develop under conditions of bombardment with high-energy particles even in films of materials with low diffusion mobility of atoms [129, 135, 136]. The extended kinetic model showed good agreement with experimental measurements of internal stresses in Ta [118], Mo [134], and Cu [137] films obtained by magnetron sputtering. In particular, it follows that, the faster the film grows, the more defects are incorporated into it, which explains the observed increase in compressive stresses. The model also made it possible to predict the experimentally observed increase in compressive stresses with a decrease in the grain size in the films. Nevertheless, the description of the evolution of internal stresses in thin films based on the kinetic model has been carried out for a very small number of materials and deposition conditions. Therefore, intensive research is required for its verification and further development.

Another type of point defects—vacancies—can also be a source of internal stresses in thin films. Films and coatings usually contain a large number of vacancies since they are deposited under highly nonequilibrium conditions. Relaxation processes occurring both during the deposition of films and after its termination lead to the ordering of their structure, in particular, to the annihilation of vacancies. This process can develop in both polycrystalline and single-crystal, as well as in amorphous films. It leads to the development of internal stresses, the sign and magnitude of which depend on the partial molar volume of vacancies, as well as on the location of the annihilation site [94]. For example, in polycrystalline films, the annihilation of a vacancy at the grain boundary located perpendicular to the film plane results in the appearance of tensile stresses. However, the annihilation of the vacancy inside the grain can, on the contrary, cause an increase in the film volume if the vacancy volume is less than the volume of the atom. This will result in the development of compressive stresses. It should be noted that, at low annealing temperatures, the stresses caused by vacancy annihilation are small. For example, the estimates made in [94] showed that the stresses caused by vacancy annihilation in Ni films subjected to annealing for 1 h at a temperature of 227°C do not exceed several tens of megapascals. At even lower temperatures, it is unlikely that this mechanism makes a significant contribution to the development of stresses in thin films.

In practice, different types of point defects are simultaneously present in films and coatings. Therefore, their influence on the development of internal stresses is complex, since different types of defects not only cause different mechanisms of stress occurrence, but also interact with each other, which can also change the stress-deformed state of the material. The modeling performed in [138] showed that the defects that occur in films can be a Frenkel defect, i.e., an interstitial atom-vacancy pair. Later molecular dynamics simulations revealed that compressive stresses in films subjected to high-energy ion bombardment can develop as a result of competing mechanisms of generating and recombining of Frenkel pairs [139].

1.4. Internal Stresses due to the Introduction of Impurities and Phase Transformations in the Film—Substrate System

Internal stresses in films and coatings can also occur due to phase transformations occurring inside them during deposition, the formation of new phases and precipitates, doping with additional elements, and the introduction of impurities. Thus, it is known that the transformation of an amorphous phase into a crystalline one leads to an increase in the density of the material [140]. Due to the rigid bond with the substrate, the films can only be compacted by reducing their thickness, which is very significant for some

materials with a variable phase state (phase change materials). For example, during crystallization of chalcogenide films (GeTe, $Ge_4Sb_1Te_5$, etc.), their thickness decreases by 8−9% [141, 142]. Such a transformation causes the development of deformations that are similar in magnitude and, consequently, tensile stresses of the order of 1 GPa and more in the film plane. A change in the phase state of films can occur both as a result of various external influences, for example, as a result of thermal annealing [143] and laser irradiation [144], as well as directly in the growth process. A similar effect has been observed, in particular, when growing Sb films [145]. Initially, these films grew in an amorphous state, but after reaching a certain critical thickness, their crystallization occurred, which was accompanied by the development of strong stresses. Another type of phase transformation occurring during the deposition of films and coatings is associated with chemical reactions taking place in them that resulted in the formation of new phases. These can be reactions caused by mutual diffusion of film and substrate atoms, or by diffusion between different layers in multilayer structures. In addition, chemical reactions of film atoms with molecules of residual gases or with embedded impurity atoms are possible.

One of the most typical examples of reactions between the chemical elements of the film and the substrate is the formation of metal silicides when metal films are deposited on a silicon substrate. In this case, the magnitude and sign of the stresses arising during the formation of a new phase cannot be unambiguously determined by calculating the difference between the volumes of the original and new phases. In general, due to the small atomic volume of silicon, the formation of silicides in thin films of metals is always accompanied by compaction of the material; i.e., this process should lead to the development of tensile stresses. Nevertheless, studies indicate that the formation of Ni_2Si [146], Pt_2Si [147], Pd_2Si [148], etc., often leads to the appearance of compressive stresses in the films, which can reach 1.5 GPa. The reason for this lies in the lower diffusion mobility of silicon atoms in comparison with metal atoms. Therefore, after the formation of a thin silicide layer between the film and the substrate, chemical reactions occur predominantly in the upper layer of the substrate adjacent to the interface with the film [149]. Therefore, it is necessary to consider changes in the volume of this phase only, i.e., to compare the volume of silicon with the volume of silicide in order to estimate the resulting deformations and stresses. Since, in this case, the volume of the new phase is larger, compressive stresses develop in the silicide layer. Studies show that the occurrence of stresses in metal films deposited on the Si substrate may be related not so much to the formation of the silicide layer itself, but rather to its transformation from an amorphous state to a crystalline one [150, 151]. Since, as was noted above, a significant compaction of

the material occurs and tensile stresses develop in the films.

Another example of the occurrence of stresses in thin films as a result of a chemical reaction is the interaction of Ti and Al with the formation of $TiAl_3$ precipitates. This phenomenon was observed, in particular, when growing Ti/Al multilayer films [152]. Since, in this case, the formation of a new phase is accompanied by a significant decrease in volume, strong tensile stresses developed in the films, which can lead to the formation of pores.

The magnitude and sign of the stresses resulting from the formation of new phases are determined by the chemical composition of the films and conditions of their deposition. Thus, the diffusion of oxygen into the Al films from the underlying layers led to the development of tensile stresses in them [80]. At the same time, the diffusion of oxygen from the $YBa_2Cu_3O_{7-x}$ layers into the Ag and Au layers caused the appearance of compressive stresses in the latter [153].

The result of interaction of the film with residual gases in the working chamber depends on their partial pressure in a complex way. Thus, with an increase in the partial pressure of oxygen during the deposition of Al films from 8×10^{-7} to 6×10^{-4} Pa, a gradual increase in the magnitude of the compressive stresses was observed in them (Fig. 6) [80]. However, a further increase in the partial pressure of oxygen led, first, to a decrease in compressive stresses and, then, at a pressure of 3×10^{-3} Pa, led to the development of tensile stresses in Al films. This behavior of the magnitude of internal stresses is explained in [80] by the fact that, at a low partial pressure, the oxygen is absorbed in the near-surface layer of the growing film in the form of interstitial atoms. This leads to compaction of the films and the appearance of compressive stresses in them. Upon reaching a pressure of 6×10^{-4} Pa, the near-surface layer of the growing film is completely saturated with oxygen. Therefore, precipitates of aluminum oxide are formed in the film that inhibit the surface diffusion of Al atoms and contribute to a decrease in the grain size. The latter, in turn, causes an increase in the relative volume of the formed grain boundaries and, as a consequence, an increase in tensile stresses arising during their formation. The result is a partial relaxation of the compressive stresses. At an oxygen pressure of 3×10^{-3} Pa, a continuous layer of aluminum oxide forms on the surface of the Al film, and the stresses in it become tensile.

An even more complicated dependence of the magnitude of internal stresses on the partial pressure of oxygen was observed upon the deposition of Cr films (Fig. 7) [154]. Since the deposition of the films was carried out at an elevated temperature (300°C), a stress evolution was observed at a low partial pressure of oxygen ($\leq 2.3 \times 10^{-6}$ Pa), which is characteristic of films with a high diffusion mobility of atoms. At first, tensile stresses arose in them, which then turned into
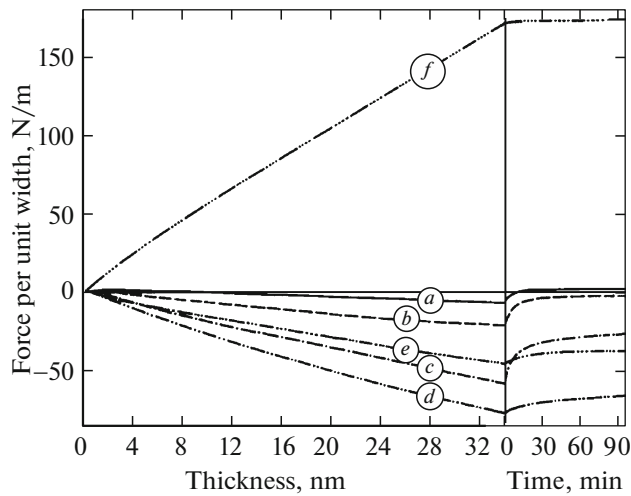
Fig. 6. Effect of partial oxygen pressure on internal stresses in Al films. The films were deposited at a partial oxygen pressure of (a) ~ 1×10^{-9}, (b) 6×10^{-6}, (c) 6×10^{-5}, (d) 6×10^{-4}, (e) 1×10^{-3}, and (f) 3×10^{-3} Pa. Adapted from [80] by courtesy of Elsevier.

Fig. 7. Influence of partial oxygen pressure on internal stresses in Cr films. Adapted from [154] by courtesy of Elsevier.

compressive ones and, at a certain thickness, again became tensile. With an increase in the partial pressure of oxygen to 3.2×10^{-5} Pa, only tensile stresses were always present in the Cr films regardless of the thickness of them. At a pressure of 3.2×10^{-4} Pa, on the contrary, the stresses were always compressive. Finally, at a partial oxygen pressure of 1.1×10^{-3} Pa, only tensile stresses developed in the films, the magnitude of which was significantly higher than at a pressure of 3.2×10^{-5} Pa. The explanation proposed by the authors of [154] for the observed dependence of internal stresses on the oxygen partial pressure largely coincides with the model described above for Al films [80]. However, in this case, it is assumed that, at a low partial pressure of oxygen, its main action is associated with the suppression of the diffusion mobility of adatoms. As a result, there is a decrease in the grain size in the film, an increase in the relative volume of grain boundaries, and, as a consequence, the development of tensile stresses. With increasing pressure, oxygen atoms are incorporated into the interstices of the crystal lattice of the surface Cr layer, which leads to the development of compressive stresses. Finally, at a pressure of 1.1×10^{-3} Pa, a continuous chromium oxide layer forms on the surface of the Cr film, which leads to the development of strong tensile stresses.

It should be noted that, today, there is no complete understanding of the factors controlling the evolution of internal stresses in thin films when the deposition parameters change. Nevertheless, the available data indicate that the introduction of impurities and phase transformations in thin films are accompanied by the development of competing mechanisms for the development of internal stresses. The contribution of each of these mechanisms to the total value of stresses significantly depends on the conditions of film growth. Therefore, it is necessary to carry out studies in a wide range of deposition parameters in order to obtain films with the required stress level.
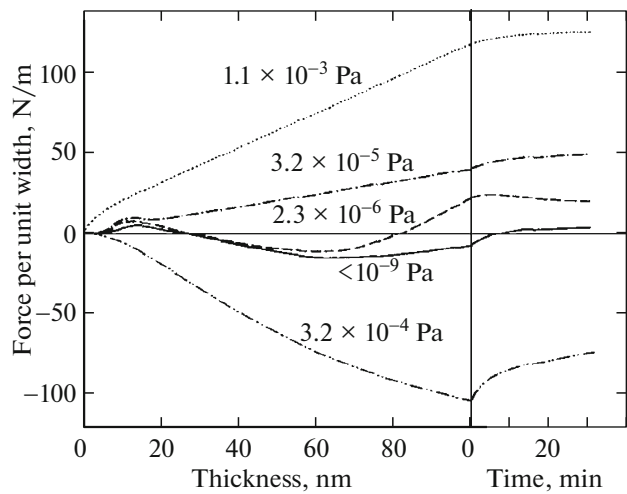
2. STRESSES DEVELOPING IN THIN-FILM STRUCTURES UNDER EXTERNAL INFLUENCES

2.1. Thermal Stresses

Thermal stresses make an important contribution to the overall stress level in thin films and coatings. Thermal stresses are external, since they are caused by temperature changes that occur, as a rule, after the end of the film deposition process. However, these stresses can be directly related to the process of film deposition, since many technologies for their growth, for example, chemical vapor deposition, thermal oxidation, etc., require the deposition of films and coatings at high temperatures (up to 1000°C or higher) [155, 156]. In addition, thermal stresses can develop during the heat treatment of films after their deposition, as well as due to temperature changes during the operation of thin films and coatings.

The reason for the development of stresses in thin-film structures with a change in temperature is the difference in the coefficients of thermal expansion (CTEs) of the film and the substrate. For example, the CTE of metal films is usually an order of magnitude higher than the CTE of a silicon substrate, which is often used for their deposition. Therefore, upon cooling of the metal film–silicon substrate structure from the synthesis temperature to room temperature, the film tends to shrink much more strongly than the substrate (Fig. 8). However, since the thickness of the

substrate is several orders of magnitude greater than the thickness of the film, the latter must be resized to match the resizing of the substrate. As a result, tensile thermal stresses arise in the film. On the contrary, when this structure is heated to a temperature exceeding the synthesis temperature, compressive stresses develop in the film. The opposite situation takes place in the case of oxide and ceramic coatings deposited on a metal substrate. Compressive stresses arise in such films and coatings during cooling, and tensile stresses arise during heating.

Upon cooling or heating of the film–substrate structure from temperature T_1 to temperature T_2, the corresponding biaxial deformation of the film is determined as follows:

$$\varepsilon = -(\alpha_f - \alpha_s)(T_2 - T_1) = -\Delta\alpha\Delta T, \qquad (20)$$

where α_f and α_s are the thermal expansion coefficients of the film and substrate, respectively.

If the temperature changes during the deposition of the film, different layers of the film will experience different deformation. Its average biaxial deformation can be calculated using the expression [94]

$$\varepsilon \approx -\Delta\alpha\left(T_2 - \frac{1}{h}\int_0^h T(z)dz\right), \qquad (21)$$

where h is the film thickness and dz is the increment in thickness. Since biaxial stresses are associated with deformation as

$$\sigma = \frac{E_f}{1 - \nu_f}\varepsilon, \qquad (22)$$

then from (20) and (22) it follows that thermal stresses are directly proportional to the change in temperature:

$$\sigma = -\frac{E_f}{(1 - \nu_f)}\Delta\alpha\Delta T. \qquad (23)$$

It should be noted that thermal stresses can be determined using (23) only in a certain temperature range in which the film undergoes only elastic deformation [157]. When thermal deformations exceed the yield strength of the film, its plastic flow begins through various mechanisms, such as dislocation slip, diffusion creep, etc. In this case, thermal stresses cannot be associated with the magnitude of elastic deformation.

Expressions (20) and (23) can be used to assess thermal deformations and stresses in multilayer structures if the total thickness of such a structure is small compared to the thickness of the substrate [94]. In this case, the calculation of stresses can be carried out separately for each layer without taking into account the influence of other layers. Thus, as in the case of a single-layer film, the parameters that determine the magnitude of thermal stresses with a change in temperature are the difference between the CTE of the given
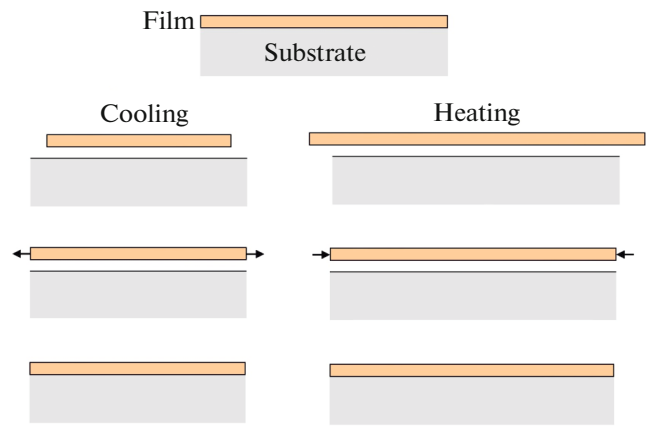
Fig. 8. Diagram illustrating the development of (left) tensile and (right) compressive thermal stresses in a film characterized by a higher CTE than the substrate.

layer and the substrate, as well as the modulus of elasticity of the layer. Therefore, the order of the layers in a multilayer structure does not affect the magnitude of thermal stresses in individual layers. In the case of a large difference between the CTE of the film and the substrate and a strong change in temperature, thermal stresses can reach very large values [158], taking into account the high values of the yield strength and strength of thin-film materials. Thus, according to [62], the cooling of Si wafers after their thermal oxidation led to the development of strong compressive stresses in the formed oxide film, the main reason for which is the difference in CTE of silicon and its oxide. Compressive stresses near the SiO_2/Si interface reached 2 GPa. The presence of stresses and deformations in the SiO_2/Si structure caused the formation of microscopic pores at the interface, which turned into macroscopic cavities in the process of cooling.

Since, as a rule, both thermal and internal stresses develop simultaneously in thin-film structures, as a result, they can both enhance (if the stresses are of the same sign) and weaken each other (if the stresses are of opposite signs). Therefore, the magnitude and sign of the stresses can change after the end of the film deposition process. Thus, it was shown that, during heteroepitaxy of SrF_2 and CaF_2 on Si (111), compressive misfit stresses develop in films [159]. However, when these systems were cooled to room temperature, the stresses became tensile due to the large difference in the CTE of the film and substrate.

2.2. Stresses in Conductive Films due to Electromigration Processes

The desire to miniaturize microelectronic devices makes it necessary to reduce the width and thickness of metal connections in them. As a result, the current density in them reaches 10^5–10^6 A/cm^2 [160, 161]. Therefore, electromigration processes have a signifi-
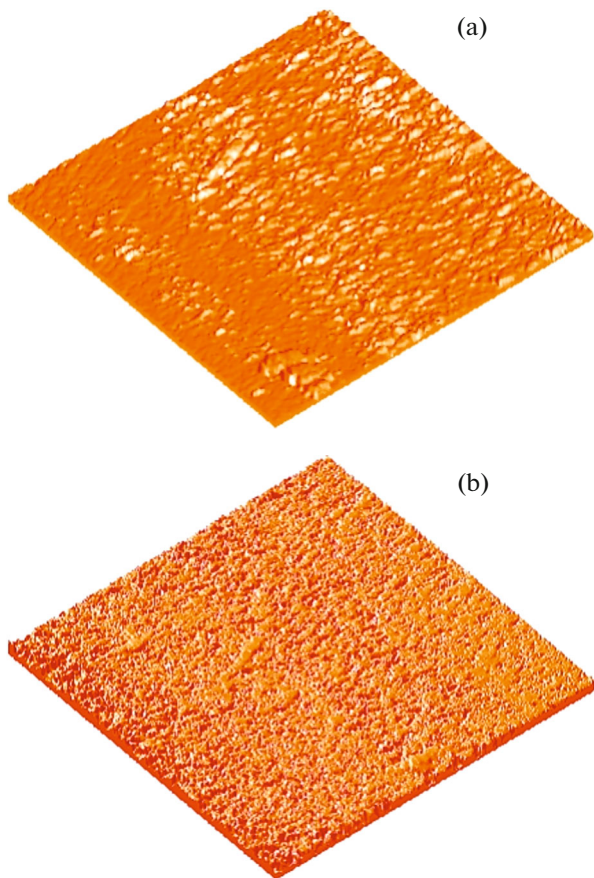
Fig. 9. Formation of (a) hillocks and (b) pores in thin Au films after passing a direct electric current with a density of $2.9 \times 10^5\,\mathrm{A/cm^2}$ for 300 h.

cant effect on the development of stresses in conductive films. In the ideal case, when there are no temperature gradients in a homogeneous thin-film conductor, ion transfer under the action of the "electron wind" by itself could not cause an increase or decrease in the density of the film material, and, therefore, the appearance of stresses in it. However, in real thin-film conductors, the divergence of the diffusing ion flow is different from zero, i.e., there is a violation of its continuity. It can be caused by a number of factors, almost all of which are associated with the microstructure of thin conductive films: gradients of defect concentration, temperature, and effective charge, as well as gradients of the diffusion coefficient or grain size [162]. Discontinuity of the mass transfer flows leads to the appearance of local regions with a higher and lower material density in the conductive films and, accordingly, compressive and tensile stresses, which in the general case can be randomly distributed along their length. Theoretical calculations have shown [163–167] that damage caused by electromigration in conductive metal films occurs when a certain critical value of stresses is exceeded. Compressive stresses cause the growth of hillocks on the surface of the film, and ten-

sile stresses cause the formation of cavities (Fig. 9). The formation of hillocks occurs due to plastic deformation of the material in a certain zone, which is initially located near the anode and, then, spreads toward the cathode. In turn, the formation and coalescence of cavities gradually lead to a shift of the cathode edge of the film towards the anode.

The study of the regularities of the development of stresses in thin films due to electromigration has been carried out in many experimental works [160, 168–171]. Thus, in [169] it was shown that the interatomic distances in thin-film Al conductors increased near the anode and decreased near the cathode under the action of the current. Thus, tensile stresses appeared at the anode, while compressive stresses arose at the cathode. At room temperature, the tensile stresses in the film were 500 MPa. At $T = 260°\mathrm{C}$, the stresses still remained tensile, but their value decreased to 50 MPa due to the compensating effect of compressive thermal stresses. It should be noted that thermal stresses are always present in conductive films, since a high-density electric current flowing through them causes an intense release of Joule heat, which leads to heating of the films [171]. As a result, thermal stresses arise in them due to the difference between the CTE of the film and the substrate. This makes it difficult to accurately determine the magnitude of the stresses caused directly by electromigration in films deposited on the substrate. Studies of electromigration in films in a free state, i.e., separated from a substrate, are carried out in order to exclude the contribution of thermal stresses. Thus, it was shown in [160] that electromigration processes in thin Pt films cause the development of local stresses, the value of which reaches 2 GPa or more. The main mechanism for relaxation of these stresses is the rapid growth of grains from 3–5 to 40 nm.

2.3. Stresses Arising due to the Influence of an Electromagnetic Field

Effects associated with the influence of an electromagnetic field can make a significant contribution to the development of stresses in thin films. First of all, these include the piezoelectric effect and electro- and magnetostriction.

The piezoelectric effect is observed in films of piezoelectrics, which are electrically neutral materials with no center of symmetry in the unit cell [172–175]. Such crystals are polarized under the influence of an external electric field, which causes their deformation, and, since piezoelectric films cannot be deformed freely due to the limitations imposed by the substrate, mechanical stresses arise in them. The value of piezoelectric deformations depends linearly on the value of the external electric field. Therefore, the stronger the field is applied to the film and the stronger its piezoelectric response, the greater the deformations and stresses will develop in it. Their magnitude and direction also depend significantly on the direction of the

external electric field. So, in the case when the field is directed perpendicular to the plane of the film, the latter will experience equiaxial compression or tension [39]. Change in the direction of the field to the opposite leads to a change in the sign of deformations and stresses.

In contrast to the piezoelectric effect, electrostriction is observed in all dielectrics and is also caused by their polarization in an external electric field [176]. However, in bulk materials, the deformation caused by electrostriction at the same field strength is several orders of magnitude less than that due to piezoelectric effect. On the other hand, deformation during electrostriction is proportional to the square of the field strength, which in thin dielectric films is inversely proportional to their thickness [177]. Therefore, the deformation of the films, and hence the corresponding stresses, can reach high values. In particular, strong stresses caused by electrostriction develop in films of anodic metal oxides, the thickness of which can be several nanometers [178−180].

It should be noted that the development of stresses in dielectric films due to electrostriction is caused by two different factors. First, as a result of polarization, uncompensated (bound) charges appear on the film surface and at its interface with the substrate. Since these bound charges on the film surface and at the interface have opposite signs, a Coulomb attraction occurs between them. As a result, the film is compressed in the normal direction to its surface. Due to the Poisson effect, this should lead to an increase in the size of the film in perpendicular directions, i.e., to its equiaxial expansion in the plane parallel to the interface. However, since the substrate prevents a change in the transverse dimensions of the film, so-called "Maxwell stresses" develop in the latter [178]:

$$\sigma_M = -\frac{\nu_f}{1 - \nu_f} \frac{\varepsilon_0 \varepsilon_d}{2} E_{el}^2, \qquad (24)$$

where ν_f is the Poisson's ratio of the film, ε_d is the permittivity of the film, ε_0 is the dielectric constant, and E_{el} is the electric field strength. As can be seen from (24), Maxwell stresses have a minus sign; i.e., they are always compressive, which follows from the geometry of the Coulomb interaction.

Second, under the action of an external electric field, molecular dipoles tend to line up along its lines of force, which also cause deformation of the dielectric film and the appearance of stresses in it. This effect is sometimes called dielectrostriction [178]. According to [178, 181], the magnitude of these stresses can be written as

$$\sigma_{ES} = -\frac{\nu}{1 - \nu} \frac{\varepsilon_0}{2} [\varepsilon_d - (\beta_1 + \beta_2)] E_{el}^2, \qquad (25)$$

where β_1 and β_2 are the electrostrictive parameters that depend on the permittivity of the film. As can be seen from (25), the sign of the stresses caused by elec-

trostriction is determined by the ratio of ε and the sum $\beta_1 + \beta_2$; i.e., these stresses can be both compressive and tensile depending on the dielectric properties of the film. Thus, electrostriction in films of anodic oxide TiO_2 led to the development of compressive stresses, the value of which reached 240 MPa [178]. At the same time, according to [179], electrostriction in anodic oxide films grown on a stainless steel substrate leads to tensile stresses. Accordingly, stresses (24) and (25) can both enhance and weaken each other. Therefore, the total value of stresses due to electrostriction depends on the ratio of σ_M and σ_{ES}. In the case of anodic oxide films on stainless steel, the Maxwell stresses are about five times higher than the stresses caused by the rearrangement of the dipoles [179]. It should also be noted that, since the deformation of the material during electrostriction is proportional to the square of the field strength, the sign of stresses and deformations does not change when the direction of the field is reversed.

A similar effect of material deformation, when the state of its magnetization changes under the influence of an external magnetic field, is called "magnetostriction." The mechanism of the development of stresses in thin-film structures caused by magnetostriction is similar to the cases of the piezoelectric effect and electrostriction described above [182, 183]. Depending on the properties of the material, magnetostriction can be positive, when the sample increases in size along the force lines of the magnetic field, and negative, when it is compressed in this direction. Accordingly, in the directions perpendicular to the lines of force, on the contrary, compression or extension occurs. Therefore, depending on the properties of the material and the direction of application of the magnetic field, the stresses in thin films caused by magnetostriction can be both compressive and tensile. Magnetostriction plays the most significant role in the occurrence of stresses in the case of strongly magnetic substances with so-called "giant magnetostriction" [184, 185]. The deformation in films of such materials can reach 10^{-2}, and the stresses can reach 1 GPa.

2.4. Stresses due to Changes in the Chemical Composition and Structure of Films

Various chemical and structural changes can occur in thin-film structures under the influence of external factors during storage and operation, which, as in the process of film growth, lead to mechanical stresses. For example, films of silicone glasses can absorb a significant amount of water from the surrounding air, and strong compressive stresses develop in them [186]. Heating these films, on the contrary, causes evaporation of moisture from them and the appearance of tensile stresses. Reversible changes in stresses in films of anodic titanium oxide can be caused by absorption and desorption of hydrogen [187]. The absorption of hydrogen by Ni films during alkaline electrolysis of

water results in the development of compressive stresses in them [188, 189].

2.5. Stresses due to Mechanical Impacts

Finally, thin films and coatings, during their operation, can be directly exposed to various mechanical influences that lead to the development of stresses in them. Thus, in recent years, researchers have shown great interest in thin-film structures on flexible substrates, which have broad prospects for use in the production of flexible LED screens, solar cells, and various microelectromechanical systems (sensors, actuators, etc.) [190−193]. During operation, such flexible thin-film structures undergo multiple bending deformations, which cause the development of inhomogeneously distributed mechanical stresses in them, which lead to their high gradients [194, 195].

The development of stresses under conditions of tribological contact in the coatings been designed to protect various parts and mechanisms from wear and tear is of special note. These include, in particular, hard ceramic coatings with increased wear resistance, which find a wide range of applications from the production of cutting tools [196, 197] to the manufacture of biomedical implants [198, 199]. In turn, metal coatings based on gold, platinum, rhodium, and palladium are used to increase the wear resistance of various contacts and connectors [200, 201]. In all cases, stresses in protective coatings arise as a result of mechanical contact interaction between bodies and can lead to delaminating and chipping of coatings [202, 203].

The occurrence of stresses during tribological contact is caused both by the force of the support reaction, which acts normally to the contact surface, and by the tangential friction force due to the relative movement of the contacting bodies. Since the surface of coatings deposited on contacting bodies always contains numerous microprotrusions of various sizes, the real contact area S_r can be several (one to five) orders of magnitude smaller than the nominal contact area S_n [204]. The average stress in the regions of contacting microprotrusions σ_{av} can be described by the following expression [205]:

$$\sigma_{av} = \sigma_n \frac{S_n}{S_r}, \tag{26}$$

where S_n is the compressive stress in the volume of the material acting in the direction of the normal to the surface. It can be seen from (26) that, even if the compressive stresses in the volume of the material are small, the average stresses in the region of the contact spots can be very high in the case of small S_r. Some of the highest microprotrusions can undergo plastic deformation, while the rest are elastically deformed [204]. In the case of relatively soft materials, an adhesive interaction occurs between the microprotrusions, which lead to the adhesion of the contacting surfaces.

The subsequent relative movement of the contacting bodies causes the formed bonds to break. In this case, the arising stresses can provide a break not along the interface, but at some depth from it; i.e., they are not adhesive, but cohesive in nature. These stresses are cyclical; i.e., the coatings are subjected to alternating cycles of tension and compression. The result is the destruction of coatings by pulling out wear particles.

CONCLUSIONS

The paper reviews modern concepts of the mechanisms of stress development in thin films and coatings during their growth, storage, and operation, as well as under various external influences. The analysis performed indicates that, although a number of mechanisms for the development of tensile stresses can act during the growth of polycrystalline films, the main reason for their occurrence is currently considered to be coalescence of islands and the appearance of excess free volume at grain boundaries. There are also a large number of causes for the development of compressive stresses in polycrystalline films; however, it is not possible to single out any prevailing mechanism, since the role of each of them for different materials and under different deposition conditions can differ significantly.

Various mechanisms of the appearance of internal stresses can act both simultaneously and sequentially during the film growth. Moreover, since some mechanisms can be replaced by others, the internal stresses in different layers of the film may differ greatly and even have opposite signs. Thus, they can both reinforce and compensate each other. A layer-by-layer analysis of stresses is required in order to identify the exact reasons for the development of stresses in the films and, accordingly, to control their stress state. Such studies can be performed primarily by continuous measurement of stresses directly during the deposition of films. Layer-by-layer measurement of stresses in thin films is also possible after the completion of their formation, for example, by using X-ray diffraction with an asymmetric recording geometry.

Analysis of the stress state arising in thin films under various external influences is also a nontrivial task. As a rule, the development of external stresses in films is a multilevel process, when the action of one external factor is often accompanied by the development of several different mechanisms of stress generation. In particular, high-temperature exposure can be simultaneously accompanied by the development of thermal stresses due to the difference between the CTE of the film and the substrate, as well as stresses caused by structural phase transformations in the film−substrate system (growth of grains and annihilation of their boundaries, the formation of new phases, etc.). The problem is further complicated by the presence of residual internal stresses in the films and the possibility of their partial relaxation under external influences. Therefore, a successful solution to the

existing problems of improving the reliability, durability, and performance of thin films and coatings is impossible without a deep understanding of the fundamental physical mechanisms underlying the generation of internal and external mechanical stresses in them.

FUNDING

CONFLICT OF INTEREST

The authors declare that they have no conflicts of interest.

REFERENCES

1. V. A. C. Haanappel, H. D. van Corbach, T. Fransen, and P. G. Gellings, Mater. Sci. Eng., A **167**, 179 (1993).
   https://doi.org/10.1016/0921-5093(93)90352-F

2. B. E. Alaca, M. T. A. Saif, and H. Sehitoglu, Acta Mater. **50**, 1197 (2002).
   https://doi.org/10.1016/S1359-6454(01)00421-9

3. P. J. J. Forschelen, A. S. J. Suiker, and O. van der Sluis, Int. J. Solids Struct. **97–98**, 284 (2016).
   https://doi.org/10.1016/j.ijsolstr.2016.07.020

4. K. Khaledi, T. Brepols, and S. Reese, Mech. Mater. **137**, 103142 (2019).
   https://doi.org/10.1016/j.mechmat.2019.103142

5. R. Stylianoua, D. Velic, W. Daves, W. Ecker, A. Stark, N. Schell, M. Tkadletz, N. Schalk, C. Czettl, and C. Mitterer, Int. J. Refract. Met. Hard Mater. **86**, 105102 (2020).
   https://doi.org/10.1016/j.ijrmhm.2019.105102

6. D. S. Balint and J. W. Hutchinson, J. Appl. Mech. **68**, 725 (2001).
   https://doi.org/10.1115/1.1388012

7. L. Lagunegrand, T. Lorriot, R. Harry, H. Wargnier, and J. M. Quenisset, Compos. Sci. Technol. **66**, 1315 (2006).
   https://doi.org/10.1016/j.compscitech.2005.10.010

8. J. W. Hutchinson, M. Y. He, and A. G. Evans, J. Mech. Phys. Solids **48**, 709 (2000).
   https://doi.org/10.1016/S0022-5096(99)00050-2

9. A. R. Shugurov and A. V. Panin, Phys. Mesomech. **13** (1–2), 9 (2010).
   https://doi.org/10.1016/j.physme.2010.03.010

10. C. Malerba, M. Valentini, R. C. L. Azanza, A. Rinaldi, and A. Mittiga, Mater. Des. **108**, 725 (2016).
    https://doi.org/10.1016/j.matdes.2016.07.019

11. D. G. Liu, L. Zheng, J. Q. Liu, L. M. Luo, and Y. C. Wu, Ceram. Int. **44**, 3644 (2018).
    https://doi.org/10.1016/j.ceramint.2017.11.115

12. S. J. Li, K. Wu, H. Z. Yuan, J. Y. Zhang, G. Liu, and J. Sun, Surf. Coat. Technol. **362**, 35 (2019).
    https://doi.org/10.1016/j.surfcoat.2019.01.088

13. R. Delmelle, S. Michotte, M. Sinnaeve, and J. Proost, Acta Mater. **61**, 2320 (2013).
    https://doi.org/10.1016/j.actamat.2013.01.003

14. X. Wang and J. J. Vlassak, Mech. Mater. **88**, 50 (2015).
    https://doi.org/10.1016/j.mechmat.2015.05.001

15. H. Wang, W. Wang, W. Yang, Y. Zhu, Z. Lin, and G. Li, Appl. Surf. Sci. **369**, 414 (2016).
    https://doi.org/10.1016/j.apsusc.2016.02.044

16. S. N. Hsiao, F. T. Yuan, S. K. Chen, A. C. Sun, S. H. Su, and K. F. Chiu, J. Magn. Magn. Mater. **398**, 275 (2016).
    https://doi.org/10.1016/j.jmmm.2015.09.034

17. M. S. Sungurov and V. A. Finkel, Tech. Phys. **63** (8), 1182 (2018).
    https://doi.org/10.1134/S1063784218080200

18. V. M. Prokhorov, E. V. Gladkikh, L. A. Ivanov, V. V. Aksenenkov, and A. N. Kirichenko, Tech. Phys. **64** (5), 654 (2019).
    https://doi.org/10.1134/S1063784219050190

19. Z. S. Ma, Y. C. Zhou, S. G. Long, and C. Lu, Surf. Coat. Technol. **207**, 305 (2012).
    https://doi.org/10.1016/j.surfcoat.2012.07.002

20. X. Zhang, M. Watanabe, and S. Kuroda, Eng. Fract. Mech. **110**, 314 (2013).
    https://doi.org/10.1016/j.engfracmech.2013.08.016

21. G.-A. Cheng, D.-Y. Han, C.-L. Liang, X.-L. Wu, and R.-T. Zheng, Surf. Coat. Technol. **228**, s328 (2013).
    https://doi.org/10.1016/j.surfcoat.2012.05.108

22. O. P. Oladijo, A. M. Venter, and L. A. Cornish, Int. J. Refract. Met. Hard Mater. **44**, 68 (2014).
    https://doi.org/10.1016/j.ijrmhm.2014.01.009

23. B. Vierneusel, L. Benker, S. Tremmel, M. Göken, and B. Merle, Thin Solid Films **638**, 159 (2017).
    https://doi.org/10.1016/j.tsf.2017.06.016

24. T. Poirié, T. Schmitt, E. Bousser, L. Martinu, and J.-E. Klemberg-Sapieha, Tribol. Int. **109**, 355 (2017).
    https://doi.org/10.1016/j.triboint.2016.12.053

25. Y. Xi, Y. Bai, K. Gao, X. Pang, H. Yang, L. Yan, and A. A. Volinsky, Ceram. Int. **44**, 15851 (2018).
    https://doi.org/10.1016/j.ceramint.2018.05.266

26. M. S. Bae, C. Park, D. Shin, S. M. Lee, and I. Yun, Solid-State Electron. **133**, 1 (2017).
    https://doi.org/10.1016/j.sse.2017.04.003

27. M. H. Hong, D. I. Shim, H. H. Cho, and H. H. Park, Appl. Surf. Sci. **446**, 160 (2018).
    https://doi.org/10.1016/j.apsusc.2018.01.283

28. T. Wang, B. Wang, A. Haque, M. Snure, E. Heller, and N. Glavin, Microelectron. Reliab. **81**, 181 (2018).
    https://doi.org/10.1016/j.microrel.2017.12.033

29. Yu. A. Boikov, I. T. Serenkov, V. I. Sakharov, and V. A. Danilov, Phys. Solid State **60** (1), 173 (2018).
    https://doi.org/10.1134/S1063783418010067

30. K. Sun, Q. Li, H. Guo, Y. Yang, and L. Li, J. Alloys Compd. **663**, 645 (2016).
    https://doi.org/10.1016/j.jallcom.2015.12.193

31. Q. Liu, W. Zhou, J. Ding, M. Xiao, Z. J. Yu, H. Xu, W. G. Mao, Y. M. Pei, F. X. Li, X. Feng, and D. N. Fang, J. Magn. Magn. Mater. **423**, 90 (2017).
    https://doi.org/10.1016/j.jmmm.2016.09.079

32. Y. Tan, K. Liang, Z. Mei, P. Zhou, Y. Liu, Y. Qi, Z. Ma, and T. Zhang, Ceram. Int. **44**, 5564 (2018).
https://doi.org/10.1016/j.ceramint.2017.12.200

33. K. Kumar, P. Arun, C. R. Kant, N. C. Mehra, L. Makinistian, and E. A. Albanesi, J. Phys. Chem. Solids **71**, 163 (2010).
https://doi.org/10.1016/j.jpcs.2009.10.013

34. B. Sarma and B. K. Sarma, J. Alloys Compd. **734**, 210 (2018).
https://doi.org/10.1016/j.jallcom.2017.11.028

35. M. L. Savchenko, N. N. Vasil'ev, A. S. Yaroshevich, D. A. Kozlov, Z. D. Kvon, N. N. Mikhailov, and S. A. Dvoretskii, Phys. Solid State **60** (4), 778 (2018).
https://doi.org/10.1134/S1063783418040285

36. W. Li, P. Li, H. Zeng, and Z. Yue, and J. Zhai, Mater. Lett. **162**, 135 (2016).
https://doi.org/10.1016/j.matlet.2015.09.137

37. Y. Wang, K. Y. Li, F. Scenini, J. Jiao, S. J. Qu, Q. Luo, and J. Shen, Surf. Coat. Technol. **302**, 27 (2016).
https://doi.org/10.1016/j.surfcoat.2016.05.034

38. S. Saha, M. Tomar, and V. Gupta, Enzyme Microb. Technol. **79−80**, 63 (2015).
https://doi.org/10.1016/j.enzmictec.2015.07.008

39. L. B. Freund and S. Suresh, *Thin Film Materials: Stress, Defect Formation and Surface Evolution* (Cambridge Univ. Press, Cambridge, 2003).

40. A. Fluri, D. Pergolesi, A. Wokaun, and T. Lippert, Phys. Rev. B **97**, 125412 (2018).
https://doi.org/10.1103/PhysRevB.97.125412

41. S. A. Kukushkin and A. V. Osipov, J. Appl. Phys. **113**, 024909 (2013).
https://doi.org/10.1063/1.4773343

42. F. S. Frank and J. H. van der Merwe, Proc. R. Soc. London, Ser. A **198**, 205 (1949).
https://doi.org/10.1098/rspa.1949.0095

43. F. C. Frank and J. H. van der Merwe, Proc. R. Soc. London, Ser. A **198**, 216 (1949).
https://doi.org/10.1098/rspa.1949.0096

44. V. A. Shchukin, A. I. Borovkov, N. N. Ledentsov, and P. S. Kop'ev, Phys. Rev. B **51**, 17767 (1995).
https://doi.org/10.1103/PhysRevB.51.17767

45. O. P. Pchelyakov, Yu. B. Bolkhovityanov, A. V. Dvurechenskii, L. V. Sokolov, A. I. Nikiforov, A. I. Yakimov, and B. Voigtländer, Semiconductors **34**, 1229 (2000).
https://doi.org/10.1134/1.1325416

46. Yu. B. Bolkhovityanov, O. P. Pchelyakov, and S. I. Chikichev, Phys.-Usp. **44**, 655 (2001).
https://doi.org/10.1070/PU2001v044n07ABEH000879

47. M. Yu. Gutkin and A. M. Smirnov, Phys. Solid State **58**, 1611 (2016).
https://doi.org/10.1134/S1063783416080138

48. H. V. Thang, S. Tosoni, and G. Pacchioni, Appl. Surf. Sci. **483**, 133 (2019).
https://doi.org/10.1016/j.apsusc.2019.03.240

49. M.-J. Casanove, A. Alimoussa, M. Schwerdtfeger, S. Gaubert, H. Moriceau, and J.-C. Villegier, Mater. Sci. Eng., B **33**, 162 (1995).
https://doi.org/10.1016/0921-5107(94)01182-6

50. Y. Obayashi and K. Shintani, J. Appl. Phys. **84**, 3141 (1998).
https://doi.org/10.1063/1.368468

51. M. Copel, M. C. Reuter, M. Horn von Hoegen, and R. M. Tromp, Phys. Rev. B **42**, 11682 (1990).
https://doi.org/10.1103/PhysRevB.42.11682

52. R. J. Asaro and W. A. Tiller, Metall. Trans. **3**, 1789 (1972).
https://doi.org/10.1007/BF02642562

53. M. A. Grinfeld, Sov. Phys.-Dokl. **31**, 831 (1986).

54. D. J. Srolovitz, Acta Metall. **37**, 621 (1989).
https://doi.org/10.1016/0001-6160(89)90246-0

55. Y. Pang and R. Huang, Phys. Rev. B **74**, 075413 (2006).
https://doi.org/10.1103/PhysRevB.74.075413

56. J. Berrehar, C. Caroli, C. Lapersonne-Meyer, and M. Schott, Phys. Rev. B **46**, 13487 (1992).
https://doi.org/10.1103/PhysRevB.46.13487

57. M. Volmer and A. Weber, Z. Phys. Chem. **119**, 277 (1926).

58. I. Lucci, S. Charbonnier, L. Pedesseau, M. Vallet, L. Cerutti, J.-B. Rodriguez, E. Tournié, R. Bernard, A. Létoublon, N. Bertru, A. Le Corre, S. Rennesson, F. Semond, G. Patriarche, L. Largeau, et al., Phys. Rev. Mater. **2**, 060401(R) (2018).
https://doi.org/10.1103/PhysRevMaterials.2.060401

59. I. N. Stranski and L. Krastanov, Sitzungsber. Akad. Wiss. Wien, Math.-Naturwiss. Kl. IIb **146**, 797 (1938).

60. D. J. Eaglesham and M. Cerullo, Phys. Rev. Lett. **64**, 1943 (1990).
https://doi.org/10.1103/PhysRevLett.64.1943

61. J. E. Prieto and I. Markov, Surf. Sci. **664**, 172 (2017).
https://doi.org/10.1016/j.susc.2017.05.018

62. M. D. Rouhani, A. M. Gue, R. Malek, G. Bouyssou, and D. Esteve, Mater. Sci. Eng., B **37**, 252 (1996).
https://doi.org/10.1016/0921-5107(95)01452-7

63. R. C. Cammarata, T. M. Trimble, and D. J. Srolovitz, J. Mater. Res. **15**, 2468 (2000).
https://doi.org/10.1557/JMR.2000.0354

64. W. D. Nix and B. M. Clemens, J. Mater. Res. **14**, 3467 (1999).
https://doi.org/10.1557/JMR.1999.0468

65. J. Leib, R. Mönig, and C. V. Thompson, Phys. Rev. Lett. **102** (25), 256101 (2009).
https://doi.org/10.1103/PhysRevLett.102.256101

66. G. Abadias, A. Fillon, J. J. Colin, A. Michel, and C. Jaouen, Vacuum **100**, 36 (2014).
https://doi.org/10.1016/j.vacuum.2013.07.041

67. E. Chason and P. R. Guduru, J. Appl. Phys. **119**, 191101 (2016).
https://doi.org/10.1063/1.4949263

68. C. Furgeaud, L. Simonot, A. Michel, C. Mastail, and G. Abadias, Acta Mater. **159**, 286 (2018).
https://doi.org/10.1016/j.actamat.2018.08.019

69. R. Koch, Surf. Coat. Technol. **204**, 1973 (2010).
https://doi.org/10.1016/j.surfcoat.2009.09.047

70. D. Magnfalt, A. Fillon, R. D. Boyd, U. Helmersson, K. Sarakinos, and G. Abadias, J. Appl. Phys. **119**, 055305 (2016).
https://doi.org/10.1063/1.4941271

71. D. L. Ma, P. P. Jing, Y. L. Gong, B. H. Wu, Q. Y. Deng, Y. T. Li, C. Z. Chen, Y. X. Leng, and N. Huang, Vacuum **160**, 226 (2019).
https://doi.org/10.1016/j.vacuum.2018.11.039

72. D. P. Adams, L. J. Parfitt, J. C. Biello, S. M. Yalisove, and Z. U. Rek, Thin Solid Films **266**, 52 (1995).
https://doi.org/10.1016/0040-6090(95)00603-6

73. C. Hua, X. Yan, J. Wei, J. Guo, J. Liu, L. Chen, L. Hei, and C. Li, Diamond Relat. Mater. **73**, 62 (2017).
https://doi.org/10.1016/j.diamond.2016.12.008

74. M. Laugier, Vacuum **31**, 155 (1981).
https://doi.org/10.1016/0042-207X(81)90007-5

75. R. C. Cammarata, Prog. Surf. Sci. **46**, 1 (1994).
https://doi.org/10.1016/0079-6816(94)90005-1

76. C. Friesen and C. V. Thompson, Phys. Rev. Lett. **89**, 126103 (2002).
https://doi.org/10.1103/PhysRevLett.89.126103

77. C. Friesen, S. C. Seel, and C. V. Thompson, J. Appl. Phys. **95**, 1011 (2004).
https://doi.org/10.1063/1.1637728

78. C. W. Pao, D. J. Srolovitz, and C. V. Thompson, Phys. Rev. B **74**, 155437 (2006).
https://doi.org/10.1103/PhysRevB.74.155437

79. R. Abermann and R. Koch, Thin Solid Films **129**, 71 (1985).
https://doi.org/10.1016/0040-6090(85)90096-3

80. R. Abermann, Thin Solid Films **186**, 233 (1990).
https://doi.org/10.1016/0040-6090(90)90145-4

81. R. Abermann, Vacuum **41**, 1279 (1990).
https://doi.org/10.1016/0042-207X(90)93933-A

82. D. W. Hoffman and J. A. Thornton, J. Vac. Sci. Technol. **20**, 355 (1982).
https://doi.org/10.1116/1.571463

83. M. Janda and O. Stefan, Thin Solid Films **112**, 127 (1984).
https://doi.org/10.1016/0040-6090(84)90490-5

84. J. A. Floro, S. J. Hearne, J. A. Hunter, P. Kotula, E. Chason, S. C. Seel, and C. V. Thompson, J. Appl. Phys. **89**, 4886 (2001).
https://doi.org/10.1063/1.1352563

85. H. Z. Yu and C. V. Thompson, Acta Mater. **67**, 189 (2014).
https://doi.org/10.1016/j.actamat.2013.12.031

86. C. V. Thompson and R. Carel, J. Mech. Phys. Solids **44**, 657 (1996).
https://doi.org/10.1016/0022-5096(96)00022-1

87. H. K. Pulker, Thin Solid Films **89**, 191 (1982).
https://doi.org/10.1016/0040-6090(82)90447-3

88. R. W. Hoffman, in *Physics of Thin Films*, Ed. by G. Hass and R.E. Thun (Academic, New York, 1966), Vol. 3, p. 211.

89. R. W. Hoffman, Thin Solid Films **34**, 185 (1976).
https://doi.org/10.1016/0040-6090(76)90453-3

90. L. B. Freund and E. Chason, J. Appl. Phys. **89**, 4866 (2001).
https://doi.org/10.1063/1.1359437

91. K. L. Johnson, K. Kendall, and A. D. Roberts, Proc. R. Soc. London, Ser. A **324**, 301 (1971).
https://doi.org/10.1098/rspa.1971.0141

92. R. Koch, J. Phys.: Condens. Matter **6**, 9519 (1994).
https://doi.org/10.1088/0953-8984/6/45/005

93. P. Chaudhari, J. Vac. Sci. Technol. **9**, 520 (1972).
https://doi.org/10.1116/1.1316674

94. M. F. Doerner and W. D. Nix, Crit. Rev. Solid State Mater. Sci. **14**, 225 (1988).
https://doi.org/10.1080/10408438808243734

95. H. J. Frost, F. Spaepen, and M. F. Ashby, Scr. Metall. **16**, 1165 (1982).
https://doi.org/10.1016/0036-9748(82)90089-8

96. R. Abermann, R. Koch, and R. Kramer, Thin Solid Films **58**, 365 (1979).
https://doi.org/10.1016/0040-6090(79)90272-4

97. F. Spaepen, Acta Mater. **48**, 31 (2000).
https://doi.org/10.1016/S1359-6454(99)00286-4

98. A. Gonzalez-González, G. M. Alonzo-Medina, A. I. Oliva, C. Polop, J. L. Sacedón, and E. Vasco, Phys. Rev. B **84**, 155450 (2011).
https://doi.org/10.1103/PhysRevB.84.155450

99. A. González-González, C. Polop, and E. Vasco, Phys. Rev. Lett. **110**, 056101 (2013).
https://doi.org/10.1103/PhysRevLett.110.056101

100. E. Chason, B. W. Sheldon, L. B. Freund, J. A. Floro, and S. J. Hearne, Phys. Rev. Lett. **88**, 156103 (2002).
https://doi.org/10.1103/PhysRevLett.88.156103

101. S. J. Tello, A. F. Bower, E. Chason, and B. W. Sheldon, Phys. Rev. Lett. **98**, 216104 (2007).
https://doi.org/10.1103/PhysRevLett.98.216104

102. E. Chason, Thin Solid Films **526**, 1 (2012).
https://doi.org/10.1016/j.tsf.2012.11.001

103. E. Chason, J. W. Shin, S. J. Hearne, and L. B. Freund, J. Appl. Phys. **111**, 083520 (2012).
https://doi.org/10.1063/1.4704683

104. E. Chason and A. F. Bower, J. Appl. Phys. **125**, 115304 (2019).
https://doi.org/10.1063/1.5085313

105. J. W. Shin and E. Chason, Phys. Rev. Lett. **103**, 056102 (2009).
https://doi.org/10.1103/PhysRevLett.103.056102

106. H. Z. Yu and C. V. Thompson, Appl. Phys. Lett. **104**, 141913 (2014).
https://doi.org/10.1063/1.4871214

107. D. Flötotto, Z. M. Wang, L. P. H. Jeurgens, and E. J. Mittemeijer, J. Appl. Phys. **118** (5), 055305 (2015).
https://doi.org/10.1063/1.4928162

108. E. Chason, A. M. Engwall, Z. Rao, and T. Nishimura, J. Appl. Phys. **123**, 185305 (2018).
https://doi.org/10.1063/1.5030740

109. S. J. Hearne and J. A. Floro, J. Appl. Phys. **97**, 014901 (2005).
https://doi.org/10.1063/1.1819972

110. E. Chason, J. W. Shin, C.-H. Chen, A. M. Engwall, C. M. Miller, S. J. Hearne, and L. B. Freund, J. Appl. Phys. **115**, 123519 (2014).
https://doi.org/10.1063/1.4870051

111. A. M. Engwall, Z. Rao, and E. Chason, Mater. Des. **110**, 616 (2016).
https://doi.org/10.1016/j.matdes.2016.07.089

112. E. Chason, A. M. Engwall, F. Pei, M. Lafouresse, U. Bertocci, G. Stafford, J. A. Murphy, C. Lenihan, and D. N. Buckley, J. Electrochem. Soc. **160** (12), D3285 (2013).
https://doi.org/10.1149/2.048312jes

113. A. M. Engwall, Z. Rao, and E. Chason, J. Electrochem. Soc. **164** (13), D828 (2017).
https://doi.org/10.1149/2.0921713jes

114. R. Koch, D. Hu, and A. K. Das, Phys. Rev. Lett. **94**, 146101 (2005).
https://doi.org/10.1103/PhysRevLett.94.146101

115. H. Windischmann, Crit. Rev. Solid State Mater. Sci. **17**, 547 (1992).
https://doi.org/10.1080/10408439208244586

116. J. A. Floro, E. Chason, R. C. Cammarata, and D. J. Srolovitz, MRS Bull. **27**, 19 (2002).
https://doi.org/10.1557/mrs2002.15

117. G. C. A. M. Janssen, Thin Solid Films **515**, 6654 (2007).
https://doi.org/10.1016/j.tsf.2007.03.007

118. G. Abadias, E. Chason, J. Keckes, M. Sebastiani, G. B. Thompson, E. Barthel, G. L. Doll, C. E. Murray, C. H. Stoessel, and L. Martinu, J. Vac. Sci. Technol., A **36**, 020801 (2018).
https://doi.org/10.1116/1.5011790

119. S. O. Mbam, S. E. Nwonu, O. A. Orelaja, U. S. Nwigwe, and X. F. Gou, Mater. Res. Express **6**, 122001 (2019).
https://doi.org/10.1088/2053-1591/ab52cd

120. P. Eh. Hovsepian, A. A. Sugumaran, Y. Purandare, D. A. L. Loch, and A. P. Ehiasarian, Thin Solid Films **562**, 132 (2014).
https://doi.org/10.1016/j.tsf.2014.04.002

121. F. Cemin, G. Abadias, T. Minea, and D. Lundin, Thin Solid Films **688**, 137335 (2019).
https://doi.org/10.1016/j.tsf.2019.05.054

122. F. M. D'Heurle and J. M. Harper, Thin Solid Films **171**, 81 (1989).
https://doi.org/10.1016/0040-6090(89)90035-7

123. J. A. Thornton and D. W. Hoffman, Thin Solid Films **171**, 5 (1989).
https://doi.org/10.1016/0040-6090(89)90030-8

124. G. Carter, J. Phys. D: Appl. Phys. **27**, 1046 (1994).
https://doi.org/10.1088/0022-3727/27/5/024

125. H. Windischmann, J. Appl. Phys. **62**, 1800 (1987).
https://doi.org/10.1063/1.339560

126. L. Romano-Brandt, E. Salvatia, E. Le Bourhis, T. Moxhama, I. P. Dolbnyac, and A. M. Korsunsky, Surf. Coat. Technol. **381**, 125142 (2020).
https://doi.org/10.1016/j.surfcoat.2019.125142

127. F. Cemin, G. Abadias, T. Minea, C. Furgeaud, F. Brisset, D. Solas, and D. Lundin, Acta Mater. **141**, 120 (2017).
https://doi.org/10.1016/j.actamat.2017.09.007

128. G. C. A. M. Janssen and J.-D. Kamminga, Appl. Phys. Lett. **85**, 3086 (2004).
https://doi.org/10.1063/1.1807016

129. J.-D. Kamminga, Th. H. de Keijser, R. Delhez, and E. J. Mittemeijer, J. Appl. Phys. **88**, 6332 (2000).
https://doi.org/10.1063/1.1319973

130. C. M. Gilmore and J. A. Sprague, Thin Solid Films **419**, 18 (2002).
https://doi.org/10.1016/S0040-6090(02)00609-0

131. J.-D. Kamminga, Th. H. de Keijser, R. Delhez, and E. J. Mittemeijer, Thin Solid Films **317**, 169 (1998).
https://doi.org/10.1016/S0040-6090(97)00614-7

132. G. Abadias and Y. Y. Tse, J. Appl. Phys. **95**, 2414 (2004).
https://doi.org/10.1063/1.1646444

133. A. Debelle, G. Abadias, A. Michel, and C. Jaouen, J. Appl. Phys. **84**, 5034 (2004).
https://doi.org/10.1063/1.1763637

134. E. Chason, M. Karlson, J. J. Colin, D. Magnfält, K. Sarakinos, and G. Abadias, J. Appl. Phys. **119** (14), 145307 (2016).
https://doi.org/10.1063/1.4946039

135. A. Fillon, G. Abadias, A. Michel, and C. Jaouen, Thin Solid Films **519**, 1655 (2010).
https://doi.org/10.1016/j.tsf.2010.07.091

136. J. J. Colin, G. Abadias, A. Michel, and C. Jaouen, Acta Mater. **126**, 481 (2017).
https://doi.org/10.1016/j.actamat.2016.12.030

137. T. Kaub, Z. Rao, E. Chason, and G. B. Thompson, Surf. Coat. Technol. **357**, 939 (2019).
https://doi.org/10.1016/j.surfcoat.2018.10.059

138. J. B. Gibson, A. N. Goland, M. Milgram, and G. H. Vineyard, Phys. Rev. **120**, 1229 (1960).
https://doi.org/10.1103/PhysRev.120.1229

139. S. Zhang, H. T. Johnson, G. J. Wagner, W. K. Liu, and K. J. Hsia, Acta Mater. **51**, 5211 (2003).
https://doi.org/10.1016/S1359-6454(03)00385-9

140. L. A. Davis, in *Metallic Glasses*, Ed. by J. J. Gilman and H. J. Leamy (Am. Soc. Metals, Metals Park, Ohio, 1978), p. 190.

141. T. Nonaka, G. Ohbayashi, Y. Toriumi, Y. Mori, and H. Hashimoto, Thin Solid Films **370**, 258 (2000).
https://doi.org/10.1016/S0040-6090(99)01090-1

142. T. P. Leervad Pedersen, J. Kalb, W. K. Njoroge, D. Wamwangi, M. Wuttig, and F. Spaepen, Appl. Phys. Lett. **79**, 3597 (2001).
https://doi.org/10.1063/1.1415419

143. B. Ben Yahia, M. S. Amara, M. Gallard, N. Burle, S. Escoubas, C. Guichet, M. Putero, C. Mocuta, M.-I. Richard, R. Chahine, C. Sabbione, M. Bernard, L. Fellouh, P. Noé, and O. Thom, Micro Nano Eng. **1**, 63 (2018).
https://doi.org/10.1016/j.mne.2018.10.001

144. W. Q. Lia, F. R. Liu, Y. Z. Zhang, G. Hana, W. N. Hana, F. Liu, and N. X. Sund, J. Non-Cryst. Solids **516**, 99 (2019).
https://doi.org/10.1016/j.jnoncrysol.2019.04.004

145. H. Horikoshi and N. Tamura, Jpn. J. Appl. Phys. **2**, 328 (1963).
https://doi.org/10.1143/JJAP.2.328

146. G. E. White and H. Chen, J. Appl. Phys. **68**, 3317 (1990).
https://doi.org/10.1063/1.346384

147. P. P. Buaud, F. M. d'Heurle, E. A. Irene, B. K. Patnaik, and N. R. Parikh, J. Vac. Sci. Technol., B **9**, 2536 (1991).
https://doi.org/10.1116/1.585688

148. P. Gergaud, O. Thomas, and B. Chenevier, J. Appl. Phys. **94**, 1584 (2003).
https://doi.org/10.1063/1.1590059

149. S.-L. Zhang and F. M. d'Heurle, Thin Solid Films **213**, 34 (1992).
https://doi.org/10.1016/0040-6090(92)90471-M

150. A. Fillon, G. Abadias, A. Michel, C. Jaouen, and P. Villechaise, Phys. Rev. Lett. **104**, 096101 (2010). https://doi.org/10.1103/PhysRevLett.104.096101

151. B. Krause, G. Abadias, C. Furgeaud, A. Michel, A. Resta, A. Coati, Y. Garreau, A. Vlad, D. Hauschild, and T. Baumbach, ACS Appl. Mater. Interfaces **11**, 39315 (2019). https://doi.org/10.1021/acsami.9b11492

152. D. S. Gardner, T. L. Michalka, P. A. Flinn, T. W. Barbee, Jr., K. C. Saraswat, and J. D. Meindl, *Proc. 2nd Int. IEEE VLSI Multilevel Interconnection Conf.* (Santa Clara, 1985), p. 102.

153. D. Winau, R. Koch, M. Weber, K.-H. Rieder, R. K. Garg, T. Schurig, and H. Koch, Appl. Phys. Lett. **61**, 279 (1992). https://doi.org/10.1063/1.107937

154. G. Thurner and R. Abermann, Vacuum **41**, 1300 (1990). https://doi.org/10.1016/0042-207X(90)93939-G

155. Y. Xu and X.-T. Yan, *Chemical Vapour Deposition: An Integrated Engineering Design for Advanced Materials* (Springer, London, 2010).

156. V. K. Tolpygo and D. R. Clarke, Acta Mater. **47**, 3589 (1999). https://doi.org/10.1016/S1359-6454(99)00216-5

157. M. Murakami, J. Vac. Sci. Technol. **9**, 2469 (1991). https://doi.org/10.1116/1.577258

158. L. Rossmann, M. Northam, B. Sarley, L. Chernova, V. Viswanathan, B. Harder, and S. Raghavan, Surf. Coat. Technol. **378**, 125047 (2019). https://doi.org/10.1016/j.surfcoat.2019.125047

159. L. J. Schowalter and W. Li, Appl. Phys. Lett. **62**, 696 (1993). https://doi.org/10.1063/1.108843

160. S. Kumar, M. T. Alam, Z. Connell, and M. A. Haque, Scr. Mater. **65**, 277 (2011). https://doi.org/10.1016/j.scriptamat.2011.04.030

161. Y. H. Oh, S. I. Kim, M. Kim, S. Y. Lee, and Y. W. Kim, Ultramicroscopy **181**, 160 (2017). https://doi.org/10.1016/j.ultramic.2017.05.018

162. F. M. d'Heurle and P. S. Ho, in *Thin Films—Interdiffusion and Reactions*, Ed. by J. M. Poate, K. N. Tu, and J. W. Mayer (Wiley, New York, 1978), p. 243.

163. R. Kirchheim, Acta Metall. Mater. **40**, 309 (1992). https://doi.org/10.1016/0956-7151(92)90305-X

164. A. Korhonen, P. Børgesen, K. N. Tu, and C. Y. Li, J. Appl. Phys. **73**, 3790 (1993). https://doi.org/10.1063/1.354073

165. L. Klinger, E. Glickman, A. Katsman, and L. Levin, Mater. Sci. Eng., B **23**, 15 (1994). https://doi.org/10.1016/0921-5107(94)90271-2

166. E. E. Glickman, Phys. Low-Dimens. Struct. **1998** (5–6), 53 (1998). https://www.elibrary.ru/item.asp?id=14009779

167. L. Filipovic, Microelectron. Reliab. **97**, 38 (2019). https://doi.org/10.1016/j.microrel.2019.04.005

168. I. A. Blech and C. Herring, Appl. Phys. Lett. **29**, 131 (1976). https://doi.org/10.1063/1.89024

169. P.-C. Wang, G. S. Cargill III, I. C. Noyan, and C.-K. Hu, Appl. Phys. Lett. **72**, 1296 (1998). https://doi.org/10.1063/1.120604

170. K. N. Tu, J. Appl. Phys. **94**, 5451 (2003). https://doi.org/10.1063/1.1611263

171. K. N. Tu, Y. Liu, and M. Li, Appl. Phys. Rev. **4**, 011101 (2017). https://doi.org/10.1063/1.4974168

172. A. Ababneh, U. Schmid, J. Hernando, J. L. Sanchez-Rajas, and H. Seidel, Mater. Sci. Eng., B **172**, 253 (2010). https://doi.org/10.1016/j.mseb.2010.05.026

173. H. Liu, F. Zeng, G. Tang, F. Pan, Appl. Surf. Sci. **270**, 225 (2013). https://doi.org/10.1016/j.apsusc.2013.01.005

174. S. Dutta, A. A. Jeyaseelan, and S. Sruthi, Thin Solid Films **562**, 190 (2014). https://doi.org/10.1016/j.tsf.2014.04.072

175. L. Yin, W. Hu, M. Wu, J. Shi, and J. Zhu, J. Mater. Sci.: Mater. Electron. **30**, 14072 (2019). https://doi.org/10.1007/s10854-019-01772-5

176. R. E. Newnham, V. Sundar, R. Yimnirun, J. Su, and Q. M. Zhang, J. Phys. Chem. B **101**, 10141 (1997). https://doi.org/10.1021/jp971522c

177. V. A. Ivanov, A. S. Sakharov, and M. E. Konyzhev, Usp. Prikl. Fiz. **1** (6), 697 (2013).

178. J.-F. Vanhumbeeck and J. Proost, Electrochim. Acta **53** (21), 6165 (2008). https://doi.org/10.1016/j.electacta.2007.11.028

179. A. H. Heuer, H. Kahn, P. M. Natishan, F. J. Martin, and L. E. Cross, Electrochim. Acta **58**, 157 (2011). https://doi.org/10.1016/j.electacta.2011.09.027

180. F. Blaffart, Q. Van Overmeere, T. Pardoen, and J. Proost, J. Solid State Electrochem. **17**, 1945 (2013). https://doi.org/10.1007/s10008-013-2036-0

181. R. M. McMeeking and C. M. Landis, J. Appl. Mech. **72**, 581 (2005). https://doi.org/10.1115/1.1940661

182. J.-Ph. Jay, F. Le Berre, S. P. Pogossian, and M. V. Indenbom, J. Magn. Magn. Mater. **322**, 2203 (2010). https://doi.org/10.1016/j.jmmm.2010.02.011

183. R. Varghese, R. Viswan, K. Joshi, S. Seifikar, Y. Zhou, J. Schwartz, and S. Priya, J. Magn. Magn. Mater. **363**, 179 (2014). https://doi.org/10.1016/j.jmmm.2014.03.076

184. S. H. Lim, H. J. Kim, S. M. Na, and S. J. Suh, J. Magn. Magn. Mater. **239**, 546 (2002). https://doi.org/10.1016/S0304-8853(01)00660-6

185. S. S. Aplesnin, A. N. Masyugin, M. N. Sitnicov, U. I. Rybina, and T. Ishibashi, J. Magn. Magn. Mater. **464**, 44 (2018). https://doi.org/10.1016/j.jmmm.2018.05.038

186. A. Shintani, S. Sugaki, and H. Nakashima, J. Appl. Phys. **51**, 4197 (1980). https://doi.org/10.1063/1.328277

187. J.-D. Kim, S.-I. Pyun, and M. Seo, Electrochim. Acta **48** (9), 1123 (2003). https://doi.org/10.1016/S0013-4686(02)00823-X

188. S. M. Kim, S. H. Jin, Y. J. Lee, and M. H. Lee, Electrochim. Acta **252**, 67 (2017). https://doi.org/10.1016/j.electacta.2017.08.157

189. J. Proost and A. Delvaux, Electrochim. Acta **322**, 134752 (2019).
https://doi.org/10.1016/j.electacta.2019.134752

190. O. Cao and J. A. Rogers, Adv. Mater. **21**, 29 (2009).
https://doi.org/10.1002/adma.200801995

191. J. A. Rogers, T. Someya, and Y. Huang, Science **327**, 1603 (2010).
https://doi.org/10.1126/science.1182383

192. X. M. Luo, B. Zhang, and G. P. Zhang, Nano Mater. Sci. **1** (3), 198 (2019).
https://doi.org/10.1016/j.nanoms.2019.02.003

193. W. Gao, Y. Zhu, Y. Wang, G. Yuan, and J. M. Liu, J. Materiomics **6**, 1 (2020).
https://doi.org/10.1016/j.jmat.2019.11.001

194. C.-C. Lee, Thin Solid Films **544**, 443 (2013).
https://doi.org/10.1016/j.tsf.2013.02.084

195. D. Faurie, P.-O. Renault, E. Le Bourhis, G. Geandier, P. Goudeau, and D. Thiaudiere, Appl. Surf. Sci. **306**, 70 (2014).
https://doi.org/10.1016/j.apsusc.2014.02.032

196. A. A. Vereschaka, S. N. Grigoriev, N. N. Sitnikov, G. V. Oganyan, and A. Batako, Surf. Coat. Technol. **332**, 198 (2017).
https://doi.org/10.1016/j.surfcoat.2017.10.027

197. K. Bobzin, T. Brögelmann, N. C. Kruppe, and M. Carlet, Surf. Coat. Technol. **385**, 125370 (2020).
https://doi.org/10.1016/j.surfcoat.2020.125370

198. A. Grill, Diamond Relat. Mater. **12**, 166 (2003).
https://doi.org/10.1016/S0925-9635(03)00018-9

199. M. Qadir, Y. Li, and C. Wen, Acta Biomater. **89**, 14 (2019).
https://doi.org/10.1016/j.actbio.2019.03.006

200. H. Tian, N. Saka, and E. Rabinowicz, Wear **142**, 57 (1991).
https://doi.org/10.1016/0043-1648(91)90152-K

201. N. K. Myshkin, V. V. Konchits, and M. Braunovich, *Electrical Contacts* (Intellekt, Dolgoprudnyi, 2008) [in Russian].

202. E. V. Torskaya, A. M. Merzin, I. V. Mosyagina, and Yu. V. Kornev, Phys. Mesomech. **21**, 475 (2018).
https://doi.org/10.1134/S1029959918060012

203. Q. Liu, T. He, W. Y. Guo, Y. Baia, Y. S. Ma, Z. D. Chang, H. B. Liu, Y. X. Zhou, F. Ding, Y. W. Sun, Z. F. Han, and J. J. Tang, Surf. Coat. Technol. **370**, 362 (2019).
https://doi.org/10.1016/j.surfcoat.2019.03.044

204. R. Colaço, in *Fundamentals of Friction and Wear on the Nanoscale*, Ed. by E. Gnecco and E. Meyer (Springer, Heidelberg, 2007), p. 453.

205. M. A. Fortes, R. Colaço, and M. F. Vaz, Wear **230** (1), 1 (1999).
https://doi.org/10.1016/S0043-1648(99)00086-1

Translated by S. Rostovtseva